A new promoter allows optogenetic vision restoration with enhanced sensitivity in macaque retina

Antoine Chaffiol, Romain P Caplette, Céline Jaillard, Elena Brazhnikova, Mélissa Desrosiers, Elisabeth Dubus, Laëtitia Duhamel, Emilie Macé, Olivier Marre, Patrick Benoit, et al.

▶ **To cite this version:**

Antoine Chaffiol, Romain P Caplette, Céline Jaillard, Elena Brazhnikova, Mélissa Desrosiers, et al.. A new promoter allows optogenetic vision restoration with enhanced sensitivity in macaque retina. Molecular Therapy, 2017, 25 (11), pp.2546-2560. 10.1016/j.ymthe.2017.07.011 . hal-01844782

HAL Id: hal-01844782

https://hal.sorbonne-universite.fr/hal-01844782

Submitted on 19 Jul 2018

HAL is a multi-disciplinary open access archive for the deposit and dissemination of scientific research documents, whether they are published or not. The documents may come from teaching and research institutions in France or abroad, or from public or private research centers.

L'archive ouverte pluridisciplinaire **HAL**, est destinée au dépôt et à la diffusion de documents scientifiques de niveau recherche, publiés ou non, émanant des établissements d'enseignement et de recherche français ou étrangers, des laboratoires publics ou privés.

Title: A new promoter allows optogenetic vision restoration with enhanced sensitivity in macaque retina

Short title: Optogenetic vision restoration in macaque retina

Author names and affiliations: Antoine Chaffiol[1,2,3*], Romain Caplette[1,2,3*], Céline Jaillard[1,2,3*], Elena Brazhnikova[1,2,3], Mélissa Desrosiers[1,2,3], Elisabeth Dubus[1,2,3], Laëtitia Duhamel[1,2,3], Emilie Macé[1,2,3], Olivier Marre[1,2,3], Patrick Benoit[4], Philippe Hantraye[5,6], Alexis-Pierre Bemelmans[5,6], Ernst Bamberg[7], Jens Duebel[1,2,3#], José-Alain Sahel[1,2,3,8,9#], Serge Picaud[1,2,3#], Deniz Dalkara[1,2,3#]

[1]INSERM, U968, Institut de la Vision, Paris, F-75012, France, [2]Sorbonne Universités, UPMC Univ Paris 06, UMR_S968, Institut de la Vision, Paris, F-75012, France, [3]CNRS UMR7210, Institut de la Vision, Paris, 75012, France, [4]Sanofi Ophthalmology Unit, 17, rue Moreau, 75012, Paris, France [5]Commissariat à l'Energie Atomique et aux Energies Alternatives (CEA), Département des Sciences du Vivant (DSV), Institut d'Imagerie Biomédicale (I2BM), MIRCen, F-92260 Fontenay-aux-Roses, France. [6]Centre National de la Recherche Scientifique (CNRS), Université Paris-Sud, Université Paris-Saclay, UMR 9199, Neurodegenerative Diseases Laboratory, F-92260 Fontenay-aux-Roses, France. [7]Department of Biophysical Chemistry, [5]Max Planck Institute of Biophysics, Frankfurt am Main, Germany [8]CHNO des Quinze-Vingts, DHU Sight Restore, INSERM-DHOS CIC, 28 rue de Charenton, 75012 Paris, France. [9]Fondation Ophtalmologique Adolphe de Rothschild, Paris, France

***** Equal First Author Contribution

[#] Equal Last Author contribution

Corresponding authors:

Jens Duebel, jens.duebel@gmail.com, Tel: 01.53.46.25.20,
Institut de la Vision, 17 rue Moreau, 75012, Paris France
José-Alain Sahel, j.sahel@gmail.com, Tel: 01.53.46.25.01,
Institut de la Vision, 17 rue Moreau, 75012, Paris France
Serge Picaud, serge.picaud@inserm.fr, Tel: 01.53.46.25.92,
Institut de la Vision, 17 rue Moreau, 75012, Paris France
Deniz Dalkara, deniz.dalkara@gmail.com, Tel: 01.53.46.25.32,
Institut de la Vision, 17 rue Moreau, 75012, Paris France

Abstract:

The majority of inherited retinal degenerations converge on the phenotype of photoreceptor cell death. In these diseases second and third order neurons are spared making it possible to restore retinal light responses using optogenetics. Viral expression of channelrhodopsin in the third order neurons under ubiquitous promoters was previously shown to restore visual function, albeit at light intensities above illumination safety thresholds. Here, we report for the first time activation of macaque retinas, up to 6 months post-injection, using channelrhodopsin – CatCh at safe light intensities. High-level Catch expression was achieved thanks to a new promoter based on the regulatory region of the gamma synuclein gene (SNCG) allowing strong expression in ganglion cells across species. Our promoter, in combination with clinically proven AAV2, provides CatCh expression in peri-foveolar ganglion cells responding robustly to light under the illumination safety thresholds for the human eye. On the contrary, the threshold of activation and the proportion of unresponsive cells were much higher when a ubiquitous promoter (CMV) was used to express CatCh. The results of our study suggest that the inclusion of optimized promoters is key in the path to clinical translation of optogenetics.

Introduction:

Inherited retinal degenerations (IRD) affect around 1 in 3000 people [1]. IRDs are a diverse group of conditions that result from mutations in any one of over two hundred and fifty different genes with the most common form being Retinitis Pigmentosa (RP) [2]. Despite the great diversity of mutations, RP converges on a phenotype of photoreceptor cell loss in later stages of the disease. Studies of post-mortem retinas from RP patients have shown that a large percentage of inner retinal neurons remain present even after photoreceptor degeneration [3]. In absence of functional photoreceptors, electrical stimulation of these inner retinal neurons was shown to enable patients to recover some visual perception, even perform some reading tasks [4]. These results collectively demonstrated that RGCs remain able to transmit information to the brain in late-stage RP [5]. However, prosthetic approaches do not yet allow sufficient resolution for face recognition or locomotion in an unknown environment [6].

As an alternative to retinal prosthesis, optogenetics can be used to restore vision by expressing optical neuromodulators such as channelrhodopsins or photochemically modified mammalian ion channels in residual retinal neurons[7–15]. Expressing channelrhodopsin in RGCs might allow spatial resolution and acuity than with current prosthetic devices. This has motivated a large body of proof-of-concept studies in rodents and other small animals, which have shown the feasibility of the approach [7–10,16–18] and a first in man Phase1 clinical trial has been initiated very recently (NCT02556736). However the use of genetically encoded opsins for vision restoration has several setbacks in terms of clinical development. First, optogenetically equipped cells require very high-level opsin expression as there is no amplification cascade behind microbial opsins[19]. Although, AAVs have a favorable safety profile in clinical gene therapy [20–23] their safety is dose dependent [24,25] limiting the injected dose. This makes uncertain our ability to obtain functional level microbial opsin expression with a safe viral dose. Second, microbial opsins require high intensity light to induce action potential firing in neurons. High intensity blue light, necessary to activate channelrhodopsin-2, might exceed the safety threshold of retinal illumination due to photochemical damage. The intensity of illumination necessary to trigger spikes depends on the number of opsin molecules expressed on the cell surface and the sensitivity of the microbial opsin. These parameters need to be considered in an animal model that resembles most closely to humans. Thus far, the work assessing feasibility of

using microbial opsins for vision restoration has been carried out in small laboratory animals such as rodents, rabbits and marmosets [7–10,26,27]. The viral doses and construct optimisations necessary to get functional optogenetic readout have not yet been investigated in macaques.

For these reasons, we studied for the first time, the safety and light intensity requirements of optogenetic vision restoration in cynomolgus macaques. AAV2 was chosen for gene delivery due to its efficacy in targeting RGCs, and the large body of knowledge using this serotype in non-human primate studies[24,28,29] and in human clinical trials [20–23,30]. To obtain functional responses at lower light intensities, we optimized several parameters: First, we used a human codon optimized CatCh, shown to be 70 times more sensitive than channelrhodopsin [31]. Second, as we are limited in the number of AAV particles we can inject into the eye, we searched for a promoter sequence to increase the efficiency of transgene expression. The promoter sequence we designed is derived from regulatory region of the human gamma-synuclein gene and in combination with AAV2 capsid leads to robust and specific transgene expression in RGCs both in mice and in non-human primates. After the vector dosing studies in blind rd1 mice, we examined the efficiency of CatCh expression in RGCs of twenty macaque eyes over a time period of 3-6 months. Our study shows for the first time CatCh expression in macaque RGCs and CatCh-mediated light responses with light intensities below illumination safety limits. Results from our study will be highly valuable in guiding viral dose and promoter choice in further clinical development of this approach and other optogenetic approaches aiming at vision restoration. Furthermore, the RGC promoter, we describe here, will benefit both basic research[32] and clinical gene therapies targeting RGCs[33].

Results:

Strong, RGC-specific expression in the mouse retina by a new promoter sequence based on regulatory region of human gamma synuclein

To identify a promoter sequence that can drive higher level gene expression in RGCs than the previously used ubiquitous promoters such as CMV, we searched for genes that are highly and exclusively expressed in RGCs [34]. Data from the literature show that gamma-synuclein is expressed both in rodent and human ganglion cells independently of the RGC type [34]. The promoter sequence of the gene however had not been described.

We thus amplified a human genomic DNA fragment of 1 kB between the +1 of the gamma synuclein gene and the untranslated 5' region downstream (Supplemental Fig. 1). This amplified region contains the promoter, but that we did not attempt any additional promoter characterization within this reagion (i.e. promoter bashing). We cloned this fragment upstream of humanized CatCh (human codon-optimized channelrhodopsin bearing the L132C mutation) in an AAV backbone. AAV2 vectors were produced with either CMV or SNCG promoter driving the expression of CatCh in fusion with GFP. Five rd1 mouse eyes were intravitreally AAV-injected with either CMV or SNCG driving expression of CatCh-GFP. Fluorescent fundus images showed higher fluorescence in all eyes injected with SNCG with respect to eyes injected with CMV (Figure. 1 A). Eyes were enucleated 8 weeks after injection and retinal flat-mounts corroborated higher intensity fluorescence with SNCG promoter compared to CMV (Figure 1 B). We evaluated strength and efficacy of gene expression in RGCs by investigating localization of expression by co-labeling with Brn3a (Figure 1 C). Brn3a is specifically expressed in RGCs and antibodies against this transcription factor are considered a reliable marker to identify and quantify RGCs [35]. Confocal microscopy images of retinal flat-mounts (Figure 1 D) and cross-sections (Figure 1 E) from SNCG-CatCh-GFP retinas showed strong GFP expression in RGCs and this expression was highly co-localized with the Brn3a labeling. No expression was noted in deeper retinal layers and in ChAT-positive amacrine cells of the RGC layer (Supplemental Fig. 2). In cell quantification of such images, we showed that the Brn3a antibody labels an equal number of RGCs on retinas transfected with either the SNCG or CMV promoter. In SNCG retinas, 57% of these Brn3a-positive RGCs were also expressing GFP whereas this proportion decreased to 21% in the CMV retinas (Figure 1 C, left). Furthermore, the GFP intensity, as quantified by area and mean immunofluorescence (Figure 1 C, right), was higher in retinas expressing GFP under SNCG promoter. The differences between SNCG and CMV retinas were statistically significant ($p<0.01$ for both Brn3a/GFP+ co-labeling and mean fluorescence values, unpaired t-tests). The greater number of GFP-expressing Brn3a-positive RGCs and the intensity of GFP expression demonstrated the efficacy of SNCG promoter to drive high-level gene expression in mouse RGCs (Figure 1 D-E). The minor percentage of Brn3a negative but GFP positive cells might belong to a class of RGCs of the accessory optic, pretectal, or hypothalamic pathways which do not stain with Brn3a [35].

Retinal and cortical responses following CatCh expression in RGCs of the rd1 retina under the SNCG promoter

To demonstrate that selective RGC targeting of CatCh-GFP can restore visual function in blind rd1 retinas (age > 12 weeks), we recorded spiking activity from RGCs using a multi-electrode array (252 electrodes MEA), 8-12 weeks after injection (Figure 2 A-E). Rd1 mice were injected at 4-8 weeks after birth with 3 doses of AAV2 encoding CatCh-GFP either under CMV or SNCG promoter. Wild-type (c57bl6) mice and uninjected rd1 mice served as controls. All rd1 retinas were recorded in presence of LAP-4. Only the wild-type controls were recorded without LAP-4. A variety of response profiles were observed in wild-type retinal ganglion cells (Supplemental Fig. 3) at an intensity of 10^{14} photons/cm^2/s. Ganglion cells from rd1 mice expressing CatCh displayed only ON-responses, between 10^{14} to 10^{17} photons/cm^2/s. Light evoked spiking activity was observed with 2 second full-field flashes (Figure 2 A-E), whereas control rd1 retinas did not show any light-elicited increase in spiking activity (data not shown). Percentage of cells responding to light was dependent on viral dose (Figure 2 A-B). Greater numbers of recorded cells responded in rd1 animals injected with the SNCG promoter at the highest AAV dose at 10^{14} photons/cm^2/s (Figure 2 A, $p<0.001$, two-way ANOVA followed by Holm-Sidak multiple comparisons). This improved sensitivity corroborates that SNCG drives higher-level CatCh expression in RGCs ensuring light-responses with lower viral load. Firing rate frequency was intensity dependent, giving rise to robust light-responses at 10^{14} photons/cm^2/s for CatCh expressed under SNCG promoter at a viral dose of $5x10^9$ vg per eye (Figure 2 A). The normalized firing rate increased with rising light intensities (Figure 2 C-D) with a representative raster plot and peri-stimulus time histogram showing increase in spike frequency during full field flashes at 480 nm in a retina expressing CatCh under control of the SNCG promoter (Figure 2 E). To demonstrate the functional efficacy in live animals, we recorded local field potentials and spiking activity in the visual cortex *in vivo*. For this experiment, another series of rd1 mice were injected with AAV2-SNCG-hCatCh-GFP, electrophysiological recordings were done in the visual cortex in response to increasing light intensities (Figure 2 F-J). VEPs were recorded on the contralateral hemisphere when stimulating the treated eye with 200 ms pulses of blue light (with light intensities up to 1.7 10^{17} photons/cm^2/s) repeated 200 times at 1 Hz (Figure 2 F-H). Due to the usage of blue light, a small

percentage of recorded RGCs in MEA experiments and some of the cortical responses could be mediated by ipRGCs[36] depolarized with the same wavelength. No VEPs were visible (flat traces) on recordings from untreated rd1 mice. CatCh-driven VEPs had shorter latencies compared to VEPs measured on wild-type mice (Figure 2 I) as described previously [12,13]. A shorter latency is expected because the phototransduction cascade and subsequent retinal computation done by the circuit are bypassed. Figure 2 F-H and J illustrate the intensity dependence of the cortical spiking responses showing that sizeable light responses are observed at light intensities as low as 10^{15} photons/cm^2/s. The latency of the light-elicited spikes in CatCh-treated rd1 mice was shorter (10.1 +/-2ms, n=3) than the mean ON latency in wild-type mice (52.98 +/-3.83 ms, n=3) as expected. These functional results clearly demonstrate that AAV-mediated expression of CatCh under the SNCG promoter can activate RGCs in the blind mouse retina and restore light sensitivity up to the visual cortex.

In vivo inflammatory responses in NHP eyes

In mouse studies, we used doses ranging from $5x10^7$ to $5x10^9$ vg/eye. We observed that using low light intensities required for minimizing phototoxicity in humans (10^{14}-10^{15} photons/cm^2/s range), the particle numbers necessary to obtain light responses on MEA and at the visual cortex were in the $5x10^8$ to $5x10^9$ vg/eye range. Since the volume of the macaque vitreous is about 100 times greater than the vitreous volume of a mouse, we decided to use the pharmacological equivalent of this dose range in our non-human primate experiments. Ten non-human primates were chosen based on absence of neutralizing antibody titers against AAV2 in their blood sera[37]. One primate was injected intravitreally with two vector doses (one eye with $1x10^{11}$ and the other with $5x10^{11}$ vg), with CatCh expressed under SNCG in fusion with GFP to monitor gene expression *in vivo* (NHP1). As GFP can be immunogenic [24], we used CatCh without fluorescent tag the remaining nine primates. 18 macaque eyes were injected intravitreally with either $1x10^{11}$ (n=5 eyes) or $5x10^{11}$ particles (n=5 eyes) or $1x10^{12}$ (n=4 eyes) of AAV2 encoding CatCh under SNCG or CMV promoter (Table 1). NHPs were followed for three to six months with regular ophthalmic exams (Figure 3 A-B). We then used Spectralis HRA-to examine the eye fundus. This instrument is built on a Confocal Scanning Laser Ophthalmoscopy (cSLO) platform that is sensitive to the fluorescence of Fluoresceine or GFP providing focused and high contrast images of the back of they eye. For the GFP

construct, green fluorescence (shown in white) detected by Spectralis HRA showed gene expression for the 5x10E11 dose starting at 1 month post-injection. Fluorescence increased up to 8 weeks post injection (Figure 3 A, middle) but was invisible for the low dose injection (Figure 3 A, left). Expression stabilized between 8-12 weeks post injection. This *in vivo* observation was consistent with CatCh expression in the retina for high viral vector doses- a result subsequently confirmed functionally and histologically in retinas where CatCh was expressed without GFP tag (see below).

Standardized uveitis nomenclature[38,39] was used to score anterior chamber flare, cells, corneal precipitates (Supplemental Fig. 4), posterior uveitis and the level of vitreal haze (Figure 3B). Between months 1 and 3, one animal in each group showed minimal to mild vitreal haze and faint to moderate posterior uveitis. All vitreal haze resolved by 4 months post-injection. Small focal vein coating resembling periphlebitis was identified in the far periphery of four animals by indirect ophthalmoscopy at two months post-injection. Fluorescent angiography was performed in these animals and showed no pathological signs (Supplemental Fig. 4 C). All of these symptoms resolved by month three after the injection. Although the number of macaques in each dosing group is too small to conclude, it seems there was no correlation between the viral dose and the inflammatory symptoms. This suggests that the inflammatory signs were in response to the procedure rather than to the viral vector or transgene product itself. Finally, none of the observed events of the inflammatory reaction throughout of five-six months observation period had influence on vision.

One eye from animal NHP3, which showed moderate posterior uveitis and minimal vitreal haze in the $5x10^{11}$ vg group (eye indicated with a white arrow) was enucleated at 3 months and examined for pathological signs related to treatment. The entire eye was fixed, sectioned and observed using nanozoomer technology allowing 40x resolution anywhere within the section (Figure 3C). No structural changes indicative of inflammation (existence of lymphocytes or plasma cells in the trabecular meshwork and the irido-corneal angle, inflammatory cells in the vitreous, or perivascular lymphocytes in the retina) were noted (Figure 3C). Despite the variable levels of vitreal haze and cells observed upon indirect ophthalmoscope evaluation at 1-2 months post-injection (Figure 3 B, C); the absence of inflammatory cells and retinal damage at three months indicate that any preceding immune reaction did not lead to permanent changes in retinal

structure. Overall the retina and anterior segments of the eye were void of any signs of damage or inflammation.

Electrophysiological recordings reveal CatCh-driven responses in RGCs around the fovea at three months post-injection

To start investigating the functionality of the CatCh expression, NHP 1 injected with AAV2-SNCG-CatCh-GFP was sacrificed three months post injection. Retinas were dissected and foveal regions were carefully cut in two halves for MEA and patch-clamp recordings because the green fluorescence attributed to GFP was maximal in this area (Figure 4 A and Figure 4 G-H). In all of our experiments, endogenous ON responses were blocked using a metabotropic glutamate receptor agonist L-(+)-2-Amino-4-phosphonobutyric acid (L-AP4) at 50µM in the bath solution. We had previously validated the L-AP4 blockade of all ON responses in wild-type retinas in both mouse, macaque and human retinas [11,15].

At the single cell level, cell-attached recordings revealed ON light-responses under 1.46 10^{16} photons/cm^2/s at 470 nm in RGCs from AAV2-SNCG-CatCh-GFP retina and in the retinas from NHP2 infected with AAV2-SNCG-CatCh without GFP which were recorded without assistance by fluorescent label (Figure 4B left and center/top right). In all patched cells under whole-cell configuration, we observed typical channelrhodopsin-evoked photocurrents consisting of a fast transient current followed by a steady-state one at a holding potential of -60mV (Figure 4B, bottom right). To define how these photocurrents control RGC activity at the population level, retinal flatmounts were recorded with the multielectrode array (MEA) technique. Spectral tuning of the firing frequency was calculated and showed highest frequency responses to 480 nm light (Figure 4 C), which corresponds to the excitation peak of ChR2 [40]. Firing rate frequency of responsive cells was intensity dependent with the maximum frequency reached at the maximum light intensity applied - 10^{17} photons/cm^2/s (Figure 4 D). Figure 4E illustrates raster plots from a single unit recording of NHP1 left eye ($5x10^{11}$ vg). Data in Figure 4F show the distribution of light responses represented as a percentage of spontaneous activity over light intensities ranging from 10^{14} to $3x10^{17}$ photons/cm^2/s for NHP1 and 2. Similar light responses were obtained for the right eye of NHP2 injected with $5x10^{11}$ vg as well as both eyes from NHP3. 45 to 90% of electrodes detected light responses in the four retinas injected with the dose of $5x10^{11}$ vg. Our results by patch clamp and MEA

indicate that the GFP tag is not required to obtain functional CatCh expression in RGCs. Eyes injected with 10^{11} vg dose showed either no responses or only a few cells were responsive suggesting that 10^{11} particles are at the threshold where we can expect reliable optogenetic activation of RGCs through expression of CatCh.

Afer MEA experiments retinal flat-mounts were stained with antibodies against channelrhodopsin [41] and Brn3a. Tissue from NHP1 was labeled with anti-GFP antibodies in green and anti-Brn3a antibodies in red (Figure 4 H). This is the only retina where we could use the RGC specific marker, Brn3a, in conjunction with an antibody indicating localization of CatCh as both Brn3a and anti-channelrhodopsin antibodies are produced in the same species. In this tissue spanning a ~1 mm square from the center of the fovea, we counted Brn3a (+) and CatCh-GFP (+) cells in half a circle with a 600 μm radius around the fovea (Figure 4 G, H). In this area, around 37% of Brn3a(+) cells were also positive for GFP (523 GFP-positive cells for 1413 Brn3a-positive cells). In the tissue from NHP 2, we counted 1351 CatCh-positive cells for one half of a retina and 455 in the contralateral retina in the region spanning 600 μm from the center of the fovea (Figure 4 I). One of the retinas from the 5 x 10^{11} -dose group was damaged following the MEA recording process and could not be used for immunofluorescence labeling. Our results indicate that at least one fourth of peri-foveolar RGCs were labeled with CatCh after an injection with 5 x 10^{11} vg dose.

CatCh-driven light responses at six months post-injection

The electrophysiological experiments done at 3-4 months post injection showed that SNCG driven CatCh expression is safe and functional at a viral dose of 5x10^{11} vg. Next, we aimed to extend the dosing range and compare SNCG to CMV promoter at a 6 months time point. This extended time point was chosen as previous studies established that after intravitreal delivery of AAV2, the transgene expression levels is stable after 6 months [29]. Based on this, we first wanted to examine if the low dose (1 x 10^{11} vg) would lead to better functional results at 6 months. NHP5 was sacrificed at 6 months post injection and MEA was used to measure light responses as described previously. A few light responsive cells were present in the right eye of this animal injected with 1 x 10^{11} vg. The contralateral eye was unresponsive confirming that 10^{11} vg dose is too low to obtain reliable optogenetic activation.

For the rest of the study, we focused on comparing CatCh mediated responses under CMV or SNCG at the two highest doses: 5 x 10^{11} vg and 10^{12} vg. Recordings were first performed on macaques injected with 5x10^{11} vg of either AAV2-CMV-CatCh (n=3 retinas) or AAV2-SNCG-CatCh (n=3 retinas). First, we compared light responses with CMV-CatCh to SNCG-CatCh using single-cell recordings. 17 out of the 52 peri-foveaolar RGCs recorded in the CMV-CatCh group were responsive to light. This ratio was as high as 18 out of 24 cells for SNCG-CatCh (Figure 5A, $p<0.001$, Chi-square). RGCs recorded in the cell-attached configuration showed significantly higher spiking frequencies for SNCG-CatCh compared to CatCh expressed under the control of CMV (Figure 5B, see averaged response in C, $p<0.001$ by t-test at 2x10^{16} photons/cm^2/s, unpaired t-test). Response latencies were also significantly shorter with SNCG than CMV (see Figure 5B, first spike latency of 12.5 ms and 32.5 ms at 10^{16} photons/cm^2/s, respectively, $p<0.01$ at 2x10^{16} photons/cm^2/s, unpaired t-test). Next, we recorded cells expressing CatCh under SNCG in whole-cell patch-clamp configuration, in order to measure CatCh-elicited inward currents at different light intensities. We found that photocurrents can be elicited at just over 10^{14} photons/cm^2/s and response amplitudes increase non-linearly with light intensity (Figure 5D). We observed photocurrents (with average τ On ~8 ms and τ Off ~16 ms at 2x10^{16} photons/cm^2/s) characterized by a transient phase followed by a robust steady-state phase under whole-cell configuration. These currents were converted into robust spiking activities under cell-attached configuration, lasting for the duration of the stimuli ranging from 20 ms to 4 s in our conditions (Figure 5E). These photocurrents and spiking activity were fast enough to follow up to 30 Hz light-pulses (Figure 5F). Next, the light intensity requirements at a population level were investigated over the entire macular region using MEA recordings. Light responses originated from the peri-foveolar area where GFP expression was observed on the retinal flatmount and their amplitude increased with stimulation intensity (Figure 5G). Figure 5H represents confocal stack projections of the same retinas labeled with ChR2 (green) antibodies. In agreement with our single-cell recordings, the number of light responsive cells over the total number of cells displaying spontaneous activity was significantly higher in retinas transduced with SNCG-CatCh compared to CMV-CatCh (Figure 5I, $p<0.001$, Chi-square). Normalized spiking frequencies across all eyes treated with SNCG (n=3) and CMV-CatCh (n=3) at a 5 x 10^{11} vg dose are shown in Figure 5J. MEA recordings over a larger population of RGCs in the macular region show the higher light-

sensitivity of RGCs expressing CatCh under SNCG promoter compared to CMV. Firing frequencies recorded across 3 retinas for each condition indicate a clear separation in the light sensitivity of the responses obtained using the two promoters.

Lastly, we investigated the utility of increasing further the viral dose to 10^{12} vg using both CMV and SNCG promoters. MEA recordings of the retina expressing CatCh under either the CMV (n=2) or the SNCG (n=2) promoters at the 10^{12} particle dose corroborate previous conclusions on the better efficacy of SNCG compared to CMV. This superiority was confirmed at both the functional level (Figure 5J) and at the cell density level (Figure 5K). Using the highest dose (10^{12} vg) slightly increased the maximum multi-unit spiking frequencies obtained with SNCG. The firing frequencies with SNCG were already very high (276,3 +/-17,9 Hz compared to 199,6 +/-40,6 Hz at 5 x 10^{11} vg under 8x10^{15} photons/cm^2/s) at 5x10^{11} vg. Moreover, the light sensitivity curves were similar for the two doses with the SNCG promoter as well as with the CMV promoter (Fig. 5J). These results clearly demonstrate the superiority of the SNCG promoter, which cannot be compensated by increasing the viral dose while using the CMV promoter.

Discussion:

There is great interest in developing optogenetics as a therapeutic modality that can be applied in humans with photoreceptor degeneration. In order to predict safety and feasibility in humans, gene delivery-related parameters need to be examined in non-human primates, which represent the human eye and immune system most closely. There are two primate models that can be used for this type of experiment, macaque and marmosets. The marmoset has a small eye with an axial length of 11 mm and AAV transduction patterns in this animal model differ from macaques in terms of cellular selectivity, spatial pattern, and depth of transduction through the retina[28]. Immune responses in the marmoset are weaker than macaques although, marmosets have an advantage over macaques for functional studies as genetic neurodegeneration models can be generated in this species[42]. As there is no non-human primate model of retinal degeneration available today, we decided to use macaques for our study. The success of optogenetics in vision restoration depends on our ability to express functional amount of the microbial opsin without eliciting immune responses to the gene delivery vector and the opsin itself. Finally, the light intensity requirements for functional activation need to fall in the range of radiation safety limits for the human eye. In view of these

requirements, we explored safety and feasibility of RGC activation with CatCh in the macaque retina. There are several AAVs that have been tested for retinal gene delivery via the intravitreal route, and some have evoked safety concerns that have not been fully addressed at this stage[25,43]. As one such example a recent study suggests that the engineered AAV variant AAV2-7m8 might be more immunogenic when used at high doses via intravitreal injections[25]. Therefore, we chose AAV2 for its known safety and efficacy in targeting RGCs in non-human primate studies [27–29] and the large body of work using this vector in human clinical trials [20–22,44,45]. High-level expression with a limited viral dose being a major parameter in obtaining functional expression, we designed a new RGC specific promoter, driving strong transgene expression in RGCs. We show that this promoter, called SNCG drives expression in twice as many RGCs compared to the ubiquitous CMV promoter. We also found that the strength of transgene expression was qualitatively stronger with SNCG promoter compared to CMV. This observation was corroborated with single cell patch experiments where higher amplitude photocurrents were recorded from cells expressing CatCh under SNCG promoter. In macaque retinas, CatCh without GFP tag localizes to the membrane in peri-foveolar RGCs and is able to mediate light-driven action potential firing in a population of RGCs with light intensities above 10^{15} photons/cm^2/s. As expected, RGCs responding to light are concentrated on the foveal center in a 500-600 µm disc where AAV2 affords efficient transduction[28]. This transduction pattern is expected to lead to a narrow visual field, albeit with good acuity. New AAV vectors and surgical procedures could help expand this limited area of transducion. Finally, we show for the first time that it is possible to stimulate CatCh expressing RGCs above 30 Hz ensuring high temporal resolution.

Gene therapeutic approaches that can provide treatments beyond the degeneration of photoreceptors are particularly important as most patients do not come to the clinic until the degenerative process has gone beyond the loss of rods and the start of cone degeneration [46]. In this regard, the results presented here provide basis for further clinical development of optogenetic reactivation of RGCs. Our study investigated the feasibility of optogenetic activation of RGCs in macaques and constitutes the basis for further investment in this direction towards improved application in patients. Because optogenetic activation relies on the resolution of the optical stimulation and the cell size, it is very likely to provide greater visual acuity than current electrical stimulations with retinal prostheses [6]. The peri-foveolar expression pattern obtained in

the non-human primate retina indicates it will be possible to optogenetically stimulate these retinal ganglion cells, making use of human retina's innate high-acuity RGC circuit. However, with current technologies it is not yet possible to achieve peripheral vision.

We found that reliable CatCh activity is seen while stimulating at an intensity threshold around 10^{15} photons/cm^2/s, with response amplitudes increasing in a light-intensity-dependent manner when using the SNCG promoter, and that significant responses can be obtained up to ~500 nm. This activation threshold is just below the radiation safety limits for the human eye[47]. By contrast, the one log unit shift in light sensitivity for the CMV promoter suggests that it could fail to elicit light responses in a safe dosing range. Moreover, potential long-term effects of expressing a light-driven channel (CatCh) with increased calcium permeability need to be taken into account when using this approach. In order to avoid potential blue light toxicity while stimulating the retina at high light intensities, developments in opsin engineering [48] and discovery[49,50] will help further refine optogenetic vision restoration strategies. In the future, we anticipate developments in both viral technologies and surgical techniques will aid in obtaining better distribution of the optogenetic protein across the primate retina. Finally for patients who still have intact bipolar cell layer, new viral technologies might also grant access to the bipolar cells of the primate retina for circuit specific insertion of G protein coupled vertebrate opsins [51–53].

Our study provides evidence that the choice of an appropriate promoter is essential in obtaining high-level microbial opsin expression compatible with illumination safety. A promoter that can drive strong gene expression in designated cells is crucial in clinical development of a strategy using a protein of foreign origin, which requires high-level expression for functional activation.

Materials and methods:

Animals

All experiments were done in accordance with the National Institutes of Health Guide for Care and Use of Laboratory Animals. The protocol was approved by the Local Animal Ethics Committees and conducted in accordance with Directive 2010/63/EU of the European Parliament. All mice used in this study were C3H/HeN (rd1 mice) or C57Bl6J mice (wild type) from Janvier Laboratories (Le Genest Saint Isle, France) or cynomolgus macaques (*macaca fasicularis*) from foreign origin.

AAV production

SNCG and CMV promoters were cloned into an AAV backbone plasmid containing human codon optimized CatCh sequence in fusion with or without GFP. The constructs all included WPRE and bovine growth hormone polyA. Recombinant AAVs were produced by the plasmid co-transfection method [54], and the resulting lysates were purified via iodixanol gradient ultracentrifugation as previously described. Briefly 40% iodixanol fraction was concentrated and buffer exchanged using Amicon Ultra-15 Centrifugal Filter Units. Vector stocks were then tittered for DNase-resistant vector genomes by real time PCR relative to a standard [55].

Injections

Mice were anesthetized with ketamine (50 mg/kg) xylazine (10 mg/kg Rompum). Injection of 1 µl stock containing 10^7 to 10^9 particles of AAV was made with direct observation of the needle in the center of the vitreous cavity. Primates were anesthetized with 10:1 mg/kg ketamine:xylazine. 100 µL of viral vector containing either 1 - 5 x 10^{11} or 10^{12} viral particles were injected into the vitreous. Ophthalmic steroid and antibiotic ointment was applied to the corneas post-injection.

Immunohistochemistry

Transduced mouse retinas were dissected and fixed in 4% paraformaldehyde for 30 min at room temperature Retinas were incubated in PBS with 1% Triton X-100, 0.5% Tween 20 and 5% BSA blocking buffer for 1 h at room temperature (RT). Retinas were incubated overnight at 4°C with polyclonal antibodies directed against GFP (Life Technologies; 1:2000) and ChAT (Millipore; 1:400); and monoclonal anti-Brn3a antibody (Millipore Chemicon; 1:100) in half diluted blocking buffer. Secondary anti-rabbit IgG, anti-mouse IgG and anti goat IgG conjugated with Alexa TM594 , Alexa TM488 and Alexa TM647 respectively (Molecular Probes; 1:500) were applied for 1 h at RT. Primate retinas were labelled with antibodies directed against Brn3a, GFP and Channelrhodopsin in similar conditions. Cell nuclei were revealed with 4',6-diamidino-2-phenylindole (Sigma-Aldrich; 10 µg/mL). Retinas were rinsed and flat-mounted in mounting medium. Cryosections of the labeled flatmounts were obtained by unmounting, cryopreserving and embedding in OCT before cryosections (15 µm).

Confocal Microscopy

Olympus FV1000 laser-scanning confocal microscope was used to acquire images sequentially, line-by-line. Step size was defined according to the Nyquist-Shannon sampling theorem. Twelve bit Images were then processed with FIJI, Z-sections were projected on a single plane using maximum intensity under Z-project function and finally converted to 8-bit RGB color mode. Efficiency of transduction was assessed by counting Brn3a (+) cells transduced with CatCh-GFP in mice and in foveal area in primate retinas. Confocal stacks through the RGC layer were acquired using the 20x objective, in four adjacent regions; above, below, to the right and left of the optic-nerve.

MEA Recordings of isolated retinas

Mice were anesthetized and sacrificed by quick cervical dislocation. Eyeballs were removed and placed in Ames medium (Sigma Aldrich A1420) bubbled with 95% O_2 and 5% CO_2 at room temperature. Eyecups were obtained under red light using binoculars by cutting around sclera, below ora serrata. Cornea and leans were then removed, and retinas were isolated and flattened. Primate eyeballs were transfered in CO2-independent medium (Life Technologies, Carlsbad, CA) after sacrifice with a lethal dose of pentobarbital. Retinas were isolated upon arrival, and the perifoveal area was cut into squared shaped pieces (approximately 4 to 5 mm) and cultured in Neurobasal medium complemented with B27 serum-free supplement (Life Technologies, Carlsbad, CA) on Transwell permeable culture support (Corning Inc., Corning, NY) as previously described (15). Primate retinal explants were left to rest in incubator for one to two days prior to MEA recordings. Isolated retinas were placed on a cellulose membrane and gently pressed against an MEA (MEA256 100/30 iR-ITO, Multichannel systems, Germany), with the RGCs facing the electrodes. The retina was continuously perfused with bubbled Ames medium at 34ºC at a rate of 1-2 ml/min during experiments. Metabotropic glutamate receptor agonist L-(+)-2-Amino-4-phosphonobutyric acid (LAP-4, Tocris Bioscience, cat No. 0103) and Glutamate antagonists 6-Cyano-7-nitroquinoxaline-2,3-dione disodium (CNQX disodium salt, Tocris Bioscience, cat No. 1045) and 3-((R)-2-Carboxypiperazin-4-yl)-propyl-1-phosphonic acid (CPP, Tocris Bioscience, cat No. 0247) were freshly diluted to concentrations of 50 µM, 25µM and 10 µM respectively and were bath-applied through the perfusion system 30 minutes prior

to recordings. Retinas were dark-adapted one hour prior to recordings. Full-field light stimuli were applied with a Polychrome V monochromator (Olympus) driven by a STG2008 stimulus generator (MCS). Output light intensities were calibrated to range from 1.10^{14} photons/cm^2/s to 1.10^{17} photons/cm^2/s. Stimuli were presented for two seconds, with ten-second intervals. Wavelength sensitivity of responses was determined by stimulating ten times, from 400 nm to 650 nm, with 10 nm steps. The order of the tested wavelengths was randomized in order to prevent any adaptation of the retina.
Raw extracellular RGC activity was amplified and sampled at 20kHz. Resulting data was stored and filtered with a 200 Hz high pass filter for subsequent offline analysis using Spike2 software v.7 (CED Co, UK). Single unit raster plots were obtained using a combination of template matching and cluster grouping based on principal component analysis of the waveforms. In our population analysis, significant responses were determined based on a z-score analysis. We estimated the mean and standard deviation of the activity prior to stimulus and considered that a response was detected if the activity exceeded the mean by more than four times the standard deviation in the 2 s after the onset or the offset of the stimulus (for a bin size of 50 ms). Error bars were calculated over the different experiments. For the responses to light at different wavelengths, we measured the response to each flash in a 1 s window after the stimulus. We then normalized the response of each cell by its maximum firing rate response. For the responses to light at different intensities, we estimated the error bars by bootstrapping over the set of recorded cells.

Two-Photon Imaging and electrophysiological recordings

A custom-made two-photon microscope equipped with a 25x water immersion objective (XLPLN25xWMP/NA1.05, Olympus) with a pulsed femto-second laser (InSight™ DeepSee™ - Newport Corporation) was used for imaging CatCh-GFP-positive retinal ganglion cells. AAV-treated retinas from rd1 mice were isolated in oxygenized (95% O_2, 5% CO_2) Ames medium (Sigma-Aldrich). For live two-photon imaging, retinas were placed in the recording chamber of the microscope, and z-stacks were acquired using the excitation laser at a wavelength of 930 nm. Images were processed offline using ImageJ. During imaging, the retina was superfused with oxygenized Ames medium.
We used an Axon Multiclamp 700B amplifier for whole-cell patch-clamp and cell-attached recordings. Patch-clamp electrodes were made from borosilicate glass (BF100-

50-10, Sutter Instruments) and pulled to 8-10 MΩ. Pipettes were filled with 112.5 mM CsMeSO4, 1 mM Mg SO4, 7.8 × 10^{-3} mM CaCl2, 0.5 mM BAPTA, 10 mM HEPES, 4 mM ATP-Na2, 0.5 mM GTP-Na3, 5 mM lidocaine N-ethyl bromide (QX314-Br) (pH 7.2). Cells were clamped at a potential of -60 mV to isolate excitatory currents. Cell-attached recordings were obtained in current-clamp configuration (current zero) with electrodes filled with AMES solution. LAP-4 was added to Ames medium during all electrophysiological recordings. Retinas were dark-adapted one hour prior to recordings.

In-vivo recordings in the visual cortex

Mice were sedated with a low dose of ketamine-xylazine injection (ketamine: 100 mg/kg and xylazine: 10 mg/kg) and then anesthetized with urethane (1.0 g/kg, 10% w/v in saline). Animals were placed in a stereotaxic holder. The temperature was maintained at 37ºC and a coverslip covered with vitamine A (Allergan) was placed on both eyes to prevent corneal dehydration. A craniotomy (1 mm^2) above V1 in the contralateral hemisphere to the treated eye, was centered 3 mm lateral and 0.5 mm rostral from the lambda point. The dura was removed and an electrode was inserted using a 3-axis micromanipulator (Sutter Instruments) with a 30° angle to the cortical surface. It was advanced 800 µm and the exposed surface was covered with agarose (1.2% in cortex buffer).

Visual stimuli were generated by a 470 nm collimated LED (model M470L3, Thorlabs) placed at 1 cm from the eye. An isolating cone ensured that the illumination was restricted to the stimulated eye. Linear multisite silicon microprobes (sixteen electrodes at 50 µm intervals) were used for recordings. For each acquisition, after averaging over the 200 trials, the electrode showing the VEP with maximal peak amplitude was selected for quantification. The stimulation consisted of 200 ms pulses of blue light repeated 200 times at 1 Hz triggered by a Digidata (Axon). Signals were analysed in Matlab using custom scripts. For local field potentials, signals were low pass filtered at 300 Hz and averaged over the 200 trials.

In vivo imaging and ophthalmic exams in non-human primates

Fluorescent images of GFP (Fundus Autofluorescence mode: excitation wavelength of 488 nm and barrier filter of 500 nm) and infrared pictures of eye fundus and OCT

images were acquired using an Spectralis HRA+OCT system (Spectralis HRA+OCT; Heidelberg Engineering, Heidelberg, Germany) after pupil dilation. Ophthalmic exams consisting of slit lamp biomicroscopy (Portable Slit Lamp model SL-14, Kowa) and indirect ophthalmoscopy (Indirect Binocular Ophthalmoscope model HK 150-1 uno, Heine) were performed on all macaques before dosing, at 2 weeks and then on monthly basis.

Histopathological studies on macaque retina

The eye from a NHP injected with the 5 x 10^{11} dose was enucleated at 3 months post-injection a needle was inserted and 0.15 - 0.3 ml of fixative was injected, until the eyeball became turgid. Eye was immersion fixed in fixative overnight and processed for making horizontal cross-sections across the entire structure. A retinal cross-section presenting all of the desired ocular structures was then imaged on a Nanozoomer (Hamamatsu, Japan).

Acknowledgements:

The authors thank the Sanofi Optovision team, Xavier Palazzi, Claire-Maelle Fovet, Valérie Fradot, Florian Senlaub for technical help and scientific advice. This work was supported by Sanofi, the Institut National de la Santé et de la Recherche Médicale (INSERM), Pierre et Marie Curie University (UPMC), the Centre National de la Recherche Scientifique (CNRS), FRM (Fondation pour la Recherche Medicale), Agence Nationale pour la Recherche Investissements d'Avenir Recherche Hospitalo-Univesritaire en santé (RHU- Light4Deaf) and (ANR: OPTIMA), the E-Rare Project (OPTOREMODE), The Foundation Fighting Blindness (Wynn-Gund translational research award), the Fédération des Aveugles de France, the city of Paris, the Regional Council of Ile-de-France, the French State program "Investissements d'Avenir" managed by the Agence Nationale de la Recherche [LIFESENSES: ANR-10-LABX-65], the ERC Starting Grant (OptogenRet, Grant Number 309776), the Deutsche Forschungsgemeinschaft (DFG) SFB 807, the Max-Planck Society and the National Institute of Health under Award Number U01NS090501.

References:

1. Bessant, DAR, Ali, RR and Bhattacharya, SS (2001). Molecular genetics and prospects for therapy of the inherited retinal dystrophies. *Current Opinion in*

Genetics and Development **11**: 307–316.
2. Wright, AF, Chakarova, CF, Abd El-Aziz, MM and Bhattacharya, SS (2010). Photoreceptor degeneration: genetic and mechanistic dissection of a complex trait. *Nature reviews. Genetics* **11**: 273–84.
3. Humayun, MS, Prince, M, de Juan, E, Barron, Y, Moskowitz, M, Klock, IB, *et al.* (1999). Morphometric analysis of the extramacular retina from postmortem eyes with retinitis pigmentosa. *Investigative ophthalmology & visual science* **40**: 143–8.
4. Humayun, MS, Dorn, JD, da Cruz, L, Dagnelie, G, Sahel, J, Stanga, PE, *et al.* (2012). Interim results from the international trial of Second Sight's visual prosthesis. *Ophthalmology* **119**: 779–88.
5. Jacobson, SG, Sumaroka, A, Luo, X and Cideciyan, A V (2013). Retinal optogenetic therapies: clinical criteria for candidacy. *Clinical genetics* **84**: 175–82.
6. Lorach, H, Goetz, G, Smith, R, Lei, X, Mandel, Y, Kamins, T, *et al.* (2015). Photovoltaic restoration of sight with high visual acuity. *Nature medicine* **21**: 476–82.
7. Bi, A, Cui, J, Ma, Y-P, Olshevskaya, E, Pu, M, Dizhoor, AM, *et al.* (2006). Ectopic expression of a microbial-type rhodopsin restores visual responses in mice with photoreceptor degeneration. *Neuron* **50**: 23–33.
8. Lagali, PS, Balya, D, Awatramani, GB, Münch, T a, Kim, DS, Busskamp, V, *et al.* (2008). Light-activated channels targeted to ON bipolar cells restore visual function in retinal degeneration. *Nature neuroscience* **11**: 667–75.
9. Greenberg, KP, Pham, A and Werblin, FS (2011). Differential targeting of optical neuromodulators to ganglion cell soma and dendrites allows dynamic control of center-surround antagonism. *Neuron* **69**: 713–20.
10. Pan, Z-H, Ganjawala, TH, Lu, Q, Ivanova, E and Zhang, Z (2014). ChR2 Mutants at L132 and T159 with Improved Operational Light Sensitivity for Vision Restoration. *PloS one* **9**: e98924.
11. Busskamp, V, Duebel, J, Balya, D, Fradot, M, Viney, TJ, Siegert, S, *et al.* (2010). Genetic Reactivation of Cone Photoreceptors Restores Visual Responses in Retinitis Pigmentosa. *Science* **329**: 413–417.
12. Tomita, H, Sugano, E, Isago, H, Hiroi, T, Wang, Z, Ohta, E, *et al.* (2009). Channelrhodopsin-2 gene transduced into retinal ganglion cells restores functional vision in genetically blind rats. *Experimental Eye Research* **90**: 429–436.
13. Caporale, N, Kolstad, KD, Lee, T, Tochitsky, I, Dalkara, D, Trauner, D, *et al.* (2011). LiGluR restores visual responses in rodent models of inherited blindness. *Molecular therapy* **19**: 1212–9.
14. Gaub, BM, Berry, MH, Holt, AE, Reiner, A, Kienzler, M a., Dolgova, N, *et al.* (2014). Restoration of visual function by expression of a light-gated mammalian ion channel in retinal ganglion cells or ON-bipolar cells. *Proceedings of the National Academy of Sciences of the United States of America* **111**: E5574-83.
15. Sengupta, A, Chaffiol, A, Macé, E, Caplette, R, Desrosiers, M, Lampič, M, *et al.* (2016). Red-shifted channelrhodopsin stimulation restores light responses in blind mice, macaque retina, and human retina. *EMBO molecular medicine* **8**: 1248–1264.
16. Doroudchi, MM, Greenberg, KP, Liu, J, Silka, K a, Boyden, ES, Lockridge, J a, *et al.* (2011). Virally delivered channelrhodopsin-2 safely and effectively restores visual function in multiple mouse models of blindness. *Molecular therapy* **19**: 1220–9.
17. Tomita, H, Sugano, E, Murayama, N, Ozaki, T, Nishiyama, F, Tabata, K, *et al.* (2014). Restoration of the Majority of the Visual Spectrum by Using Modified Volvox

Channelrhodopsin-1. *Molecular Therapy* **22**: 1434–1440.
18. Macé, E, Caplette, R, Marre, O, Sengupta, A, Chaffiol, A, Barbe, P, *et al.* (2015). Targeting channelrhodopsin-2 to ON-bipolar cells with vitreally administered AAV Restores ON and OFF visual responses in blind mice. *Molecular therapy : the journal of the American Society of Gene Therapy* **23**: 7–16.
19. Busskamp, V and Roska, B (2011). Optogenetic approaches to restoring visual function in retinitis pigmentosa. *Current opinion in neurobiology* **21**: 942–6.
20. Bainbridge, JWB, Smith, AJ, Barker, SS, Robbie, S, Henderson, R, Balaggan, K, *et al.* (2008). Effect of gene therapy on visual function in Leber's congenital amaurosis. *The New England journal of medicine* **358**: 2231–9.
21. Cideciyan, A V, Aleman, TS, Boye, SL, Schwartz, SB, Kaushal, S, Roman, AJ, *et al.* (2008). Human gene therapy for RPE65 isomerase deficiency activates the retinoid cycle of vision but with slow rod kinetics. *Proceedings of the National Academy of Sciences of the United States of America* **105**: 15112–7.
22. Maguire, AM, Simonelli, F, Pierce, EA, Pugh, EN, Mingozzi, F, Bennicelli, J, *et al.* (2008). Safety and efficacy of gene transfer for Leber's congenital amaurosis. *The New England journal of medicine* **358**: 2240–8.
23. MacLaren, RE, Groppe, M, Barnard, AR, Cottriall, CL, Tolmachova, T, Seymour, L, *et al.* (2014). Retinal gene therapy in patients with choroideremia: initial findings from a phase 1/2 clinical trial. *The Lancet* **383**: 1129–1137.
24. Vandenberghe, LH, Bell, P, Maguire, AM, Cearley, CN, Xiao, R, Calcedo, R, *et al.* (2011). Dosage thresholds for AAV2 and AAV8 photoreceptor gene therapy in monkey. *Science translational medicine* **3**: 88ra54.
25. Ramachandran, PS, Lee, V, Wei, Z, Song, JY, Casal, G, Cronin, T, *et al.* (2016). Evaluation of Dose and Safety of AAV7m8 and AAV8BP2 in the Non-Human Primate Retina. *Human gene therapy*doi:10.1089/hum.2016.111.
26. Sugano, E, Isago, H, Wang, Z, Murayama, N, Tamai, M and Tomita, H (2011). Immune responses to adeno-associated virus type 2 encoding channelrhodopsin-2 in a genetically blind rat model for gene therapy. *Gene therapy* **18**: 266–274.
27. Ivanova, E, Hwang, G-S, Pan, Z-H and Troilo, D (2010). Evaluation of AAV-mediated expression of Chop2-GFP in the marmoset retina. *Investigative ophthalmology & visual science* **51**: 5288–96.
28. Yin, L, Greenberg, K, Hunter, JJ, Dalkara, D, Kolstad, KD, Masella, BD, *et al.* (2011). Intravitreal injection of AAV2 transduces macaque inner retina. *Investigative ophthalmology & visual science* **52**: 2775–83.
29. Maclachlan, TK, Lukason, M, Collins, M, Munger, R, Isenberger, E, Rogers, C, *et al.* (2011). Preclinical safety evaluation of AAV2-sFLT01- a gene therapy for age-related macular degeneration. *Molecular therapy* **19**: 326–34.
30. Bennett, J, Ashtari, M, Wellman, J, Marshall, KA, Cyckowski, LL, Chung, DC, *et al.* (2012). AAV2 Gene Therapy Readministration in Three Adults with Congenital Blindness. *Science Translational Medicine* **4**: 120ra15-120ra15.
31. Kleinlogel, S, Feldbauer, K, Dempski, RE, Fotis, H, Wood, PG, Bamann, C, *et al.* (2011). Ultra light-sensitive and fast neuronal activation with the Ca^2+-permeable channelrhodopsin CatCh. *Nature neuroscience* **14**: 513–8.
32. Yin, L, Masella, B, Dalkara, D, Zhang, J, Flannery, JG, Schaffer, D V, *et al.* (2014). Imaging light responses of foveal ganglion cells in the living macaque eye. *The Journal of neuroscience : the official journal of the Society for Neuroscience* **34**: 6596–605.
33. Feuer, WJ, Schiffman, JC, Davis, JL, Porciatti, V, Gonzalez, P, Koilkonda, RD, *et al.*

(2016). Gene Therapy for Leber Hereditary Optic Neuropathy. *Ophthalmology* **123**: 558–570.
34. Surgucheva, I, Weisman, AD, Goldberg, JL, Shnyra, A and Surguchov, A (2008). Gamma-synuclein as a marker of retinal ganglion cells. *Molecular vision* **14**: 1540–1548.
35. Quina, LA, Pak, W, Lanier, J, Banwait, P, Gratwick, K, Liu, Y, *et al.* (2005). Brn3a-expressing retinal ganglion cells project specifically to thalamocortical and collicular visual pathways. *The Journal of neuroscience : the official journal of the Society for Neuroscience* **25**: 11595–11604.
36. Allen, AE, Storchi, R, Martial, FP, Bedford, RA and Lucas, RJ (2017). Melanopsin Contributions to the Representation of Images in the Early Visual System. *Current Biology* **27**: 1623–1632.e4.
37. Kotterman, MA, Yin, L, Strazzeri, JM, Flannery, JG, Merigan, WH and Schaffer, D V (2015). Antibody neutralization poses a barrier to intravitreal adeno-associated viral vector gene delivery to non-human primates. *Gene therapy* **22**: 1–11.
38. Nussenblatt, RB, Palestine, AG, Chan, CC and Roberge, F (1985). Standardization of vitreal inflammatory activity in intermediate and posterior uveitis. *Ophthalmology* **92**: 467–471.
39. Jabs, DA, Nussenblatt, RB and Rosenbaum, JT (2005). Standardization of uveitis nomenclature for reporting clinical data. Results of the First International Workshop. *American journal of ophthalmology* **140**: 509–516.
40. Nagel, G, Szellas, T, Huhn, W, Kateriya, S, Adeishvili, N, Berthold, P, *et al.* (2003). Channelrhodopsin-2, a directly light-gated cation-selective membrane channel. *Proceedings of the National Academy of Sciences of the United States of America* **100**: 13940–5.
41. Kleinlogel, S, Terpitz, U, Legrum, B, Gökbuget, D, Boyden, ES, Bamann, C, *et al.* (2011). A gene-fusion strategy for stoichiometric and co-localized expression of light-gated membrane proteins. *Nature Methods* **8**: 1083–1088.
42. Belmonte, JCI, Callaway, EM, Churchland, P, Caddick, SJ, Feng, G, Homanics, GE, *et al.* (2015). Brains, Genes, and Primates. *Neuron* **86**: 617–631.
43. Dalkara, D, Byrne, LC, Klimczak, RR, Visel, M, Yin, L, Merigan, WH, *et al.* (2013). In vivo-directed evolution of a new adeno-associated virus for therapeutic outer retinal gene delivery from the vitreous. *Science translational medicine* **5**: 189ra76.
44. MacLaren, RE, Groppe, M, Barnard, AR, Cottriall, CL, Tolmachova, T, Seymour, L, *et al.* (2014). Retinal gene therapy in patients with choroideremia: Initial fi ndings from a phase 1/2 clinical trial. *The Lancet* **383**: 1129–1137.
45. Bennett, J, Wellman, J, Marshall, KA, Mccague, S, Ashtari, M, Distefano-Pappas, J, *et al.* (2016). Safety and durability of eff ect of contralateral-eye administration of AAV2 gene therapy in patients with childhood-onset blindness caused by RPE65 mutations: a follow-on phase 1 trial. *The Lancet* **388**: 661–672.
46. Byrne, LC, Dalkara, D, Luna, G, Fisher, SK, Clérin, E, Sahel, J, *et al.* (2015). Viral-mediated RdCVF and RdCVFL expression protects cone and rod photoreceptors in retinal degeneration. *Journal of Clinical Investigation* **125**: 105–116.
47. Wu, J, Seregard, S and Algvere, P V. Photochemical damage of the retina. *Survey of ophthalmology* **51**: 461–81.
48. Lin, JY, Knutsen, PM, Muller, A, Kleinfeld, D and Tsien, RY (2013). ReaChR: a red-shifted variant of channelrhodopsin enables deep transcranial optogenetic excitation. *Nature neuroscience* **16**: 1499–508.
49. Klapoetke, NC, Murata, Y, Kim, SS, Pulver, SR, Birdsey-Benson, A, Cho, YK, *et al.*

(2014). Independent optical excitation of distinct neural populations. *Nature methods* **11**: 338–46.
50. Chuong, AS, Miri, ML, Busskamp, V, Matthews, G a C, Acker, LC, Sørensen, AT, *et al.* (2014). Noninvasive optical inhibition with a red-shifted microbial rhodopsin. *Nature neuroscience* **17**: 1123–1129.
51. van Wyk, M, Pielecka-Fortuna, J, Löwel, S and Kleinlogel, S (2015). Restoring the ON Switch in Blind Retinas: Opto-mGluR6, a Next-Generation, Cell-Tailored Optogenetic Tool. *PLOS Biology* **13**: e1002143.
52. Cehajic-Kapetanovic, J, Eleftheriou, C, Allen, AE, Milosavljevic, N, Pienaar, A, Bedford, R, *et al.* (2015). Restoration of Vision with Ectopic Expression of Human Rod Opsin. *Current Biology*: 1–12doi:10.1016/j.cub.2015.07.029.
53. Gaub, BM, Berry, MH, Holt, AE, Isacoff, EY and Flannery, JG (2015). Optogenetic Vision Restoration Using Rhodopsin for Enhanced Sensitivity. *Molecular therapy : the journal of the American Society of Gene Therapy* **23**: 1562–71.
54. Choi, VW, Asokan, A, Haberman, R a and Samulski, RJ (2007). Production of recombinant adeno-associated viral vectors. *Current protocols in human genetics / editorial board, Jonathan L. Haines ... [et al.]* **Chapter 12**: Unit 12.9.
55. Aurnhammer, C, Haase, M, Muether, N, Hausl, M, Rauschhuber, C, Huber, I, *et al.* (2012). Universal real-time PCR for the detection and quantification of adeno-associated virus serotype 2-derived inverted terminal repeat sequences. *Human gene therapy methods* **23**: 18–28.

Figure legends:

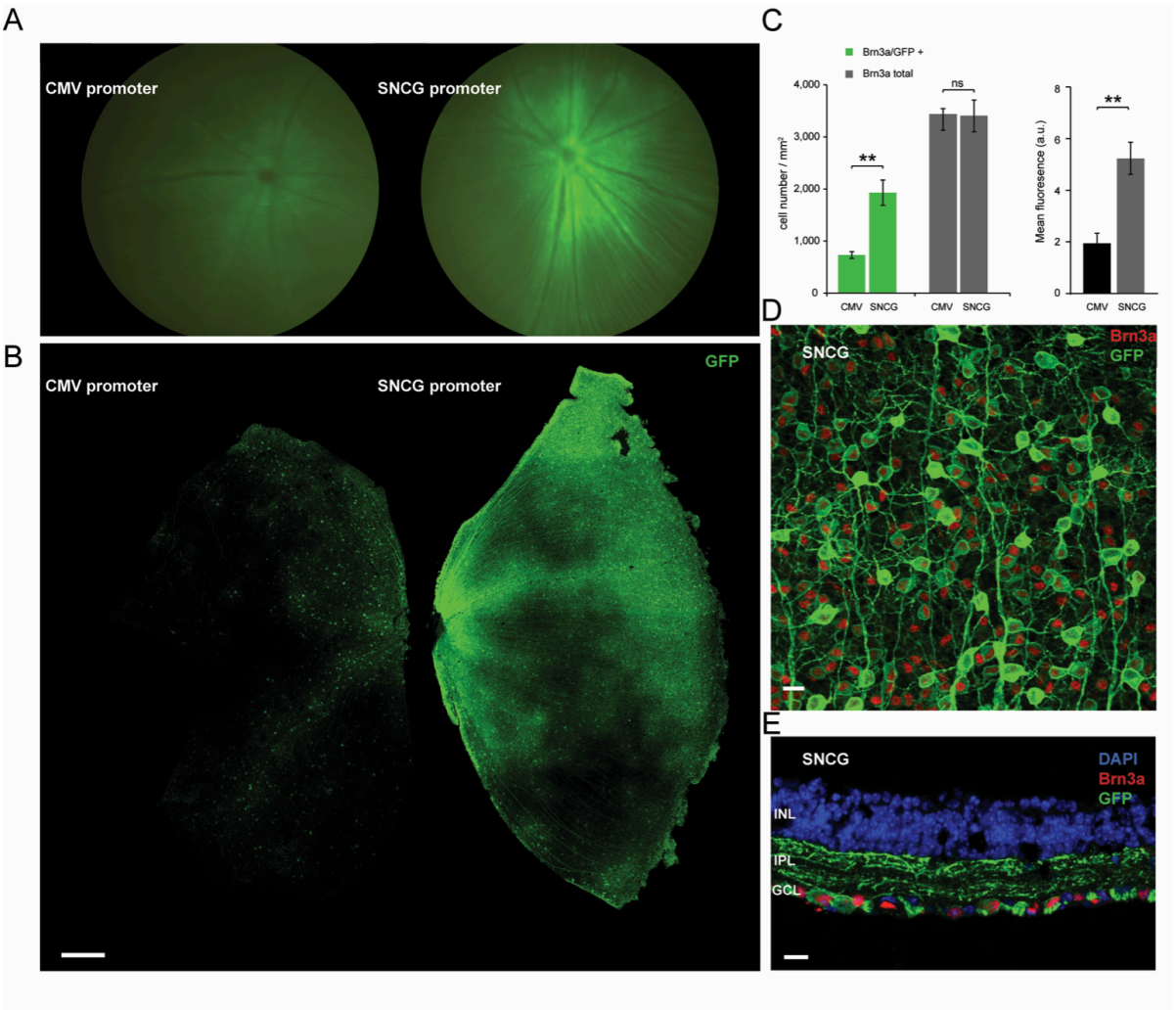

Figure 1- SNCG promoter drives higher-level hCatCh-GFP expression than CMV promoter in mouse RGCs

A) Fundus image of representative rd1 mouse retinae injected with $5x10^9$ vg of either AAV2-CMV-hCatCh-GFP (left) or AAV2-SNCG-hCatCh-GFP (right). B) Retinal flat-mounts obtained from the same injection series showing CatCh-GFP fluorescence obtained under the CMV promoter (left) and the SNCG promoter (right). Scale bar: 300 µm. C) Quantification of Brn3a-positive, GFP-positive and double labeled cells in rd1 mouse retina injected with either AAV2-SNCG-hCatCh-GFP or AAV2-CMV-hCatCh-GFP. Confocal stack projections across the ganglion cell layer for cell counts over chosen fields in the central and in peripheral regions of the retina. Regions were chosen in each quadrant and cell-counts were averaged to obtain Brn3a-positive, GFP-positive and co-labeled

cells per mm^2. Mean fluorescence values were measured over the same areas using the same number of z-stacks. Error bars represent SEM. D) Representative confocal stack projection across the RGC layer of rd1 mouse retina transduced with SNCG-CatCh-GFP, co-labeled with Brn3a (red) and anti-GFP (green) antibodies. E) Cross-sections obtained from one representative retinal flat-mount in the SNCG-CatCh-GFP injected retinas co-labeled with Bnr3a (red) and anti-GFP (green) and nuclei were labeled with DAPI (blue). Scale bars (D, E): 10 μm.

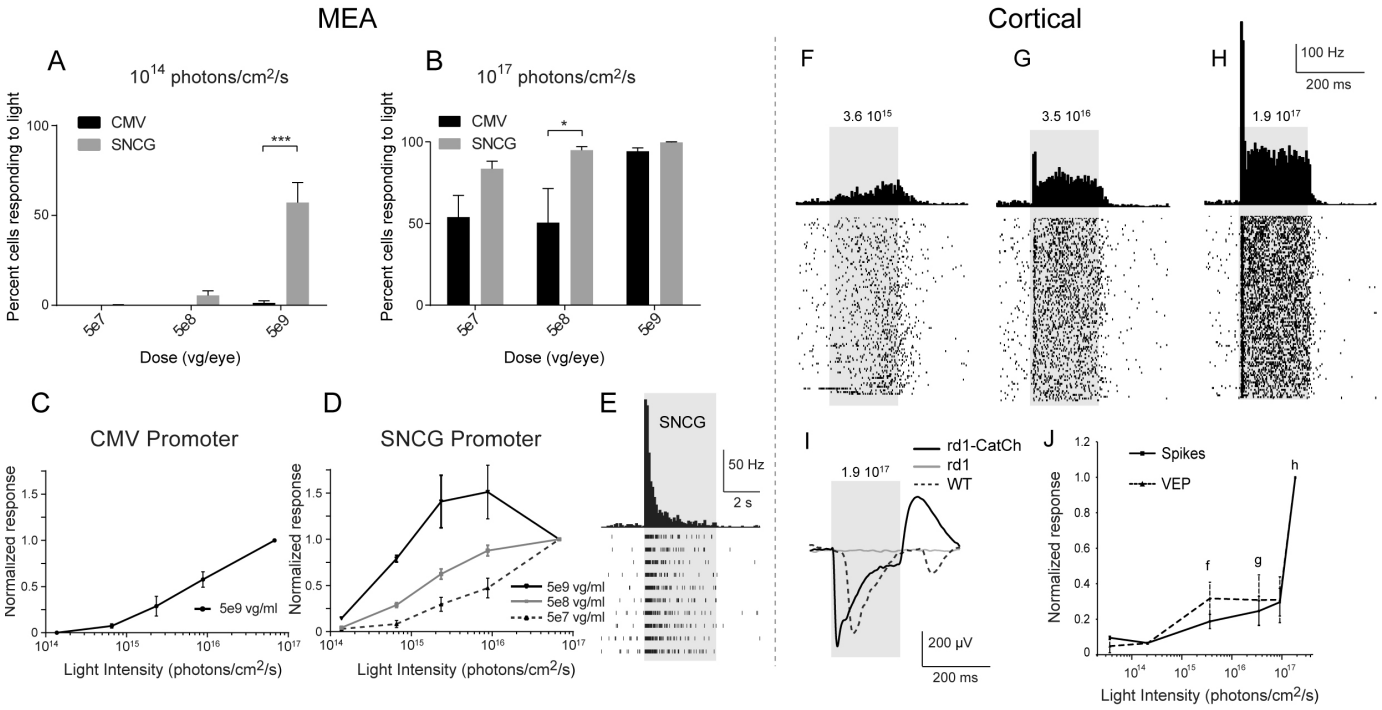

Figure 2- Functional CatCh responses in the retinas and cortex of rd1 mice

Percentages of cells with a spontaneous activity showing a light response at 480nm under either A) 10^{14} photons/cm^2/s or B) 10^{17} photons/cm^2/s in retinas expressing CatCh under control of CMV (black) or SNCG (grey) at 5x10^7, 5x10^8 and 5x10^9 vg per eye (n=4). C) Response amplitude (normalized to the response obtained at maximum luminance) as a function of light intensity in retinas expressing CatCh under control of CMV promoter at 5x10^9 viral particle dose (n=4, 155 cells) D) Response amplitude (normalized to the response obtained at maximum luminance) as a function of light intensity in retinas expressing CatCh under control of SNCG promoter at 5x10^7 viral particle dose (light grey, n=4 retinas, 158 cells), 5x10^8 (dark grey, n=4 retinas, 221 cells) and 5x10^9 (black, n=4 retinas, 261 cells) viral particles (vg) per eye. E) Raster plots and peri-stimulus time histogram (PSTH) showing the light response or increase in spike frequency during full field flashes at 480 nm in a retina expressing CatCh under control of the SNCG promoter. Note that with the SNCG promoter that the curve is reaching a plateau at the maximum AAV vector dose. (F, G, H) PSTHs (top) and corresponding raster plots (bottom) of visual cortex neurons of rd1 mice expressing SNCG-CatCh in response to 475 nm full field flashes at 3 different increasing light intensities (10^{15}, 10^{16} and 10^{17} photons/cm^2/s). I) Comparison of Visually Evoked potentials (VEPs) recorded in SNCG-CatCh treated rd1 retinas with the 5x10^9 vg dose, compared to untreated rd1 retinas and wild-type mouse retinas. J) Normalized cortical activity (spikes and VEP) as a function of light intensities at 475 nm (n=3 mice). Error bars represent SEM.

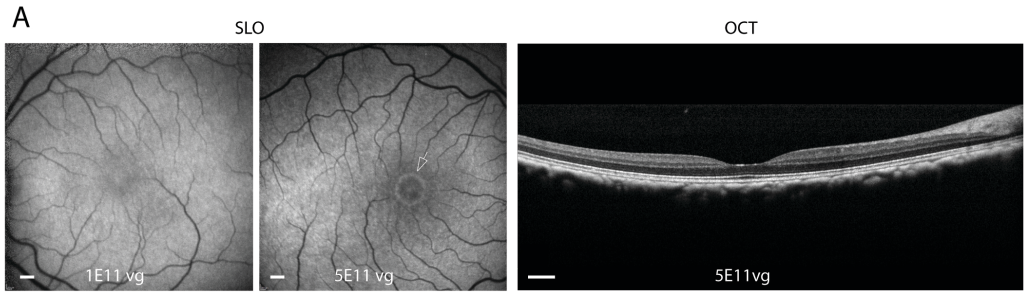
A
SLO
OCT
1E11 vg
5E11 vg
5E11vg

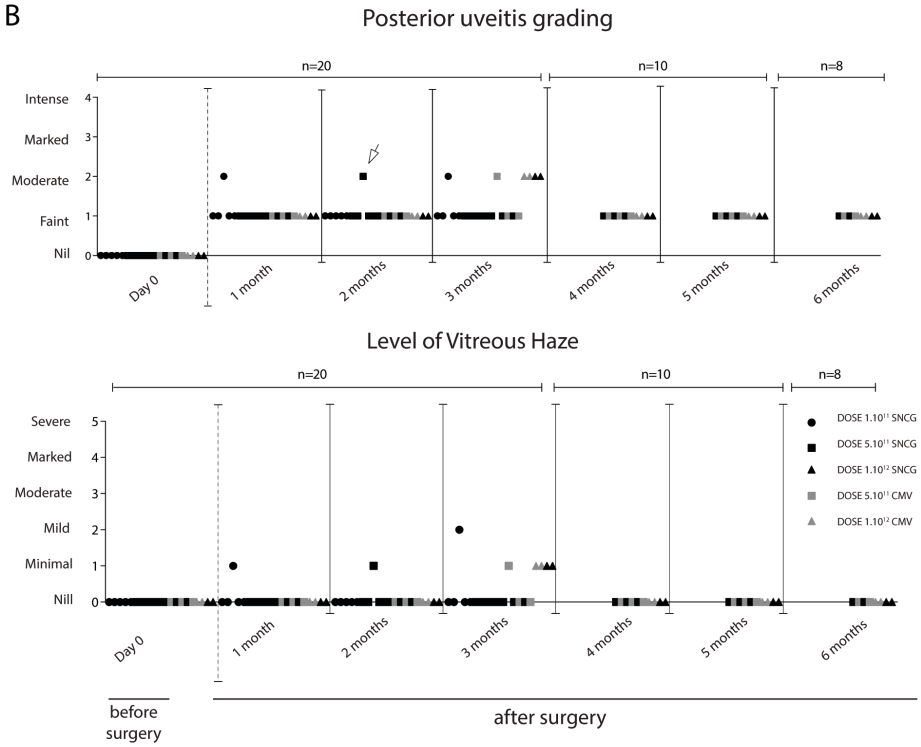
B
Posterior uveitis grading
n=20
n=10
n=8
Intense
Marked
Moderate
Faint
Nil
Day 0
1 month
2 months
3 months
4 months
5 months
6 months
Level of Vitreous Haze
Severe
Marked
Moderate
Mild
Minimal
Nill
DOSE 1.10¹¹ SNCG
DOSE 5.10¹¹ SNCG
DOSE 1.10¹² SNCG
DOSE 5.10¹¹ CMV
DOSE 1.10¹² CMV
before surgery
after surgery

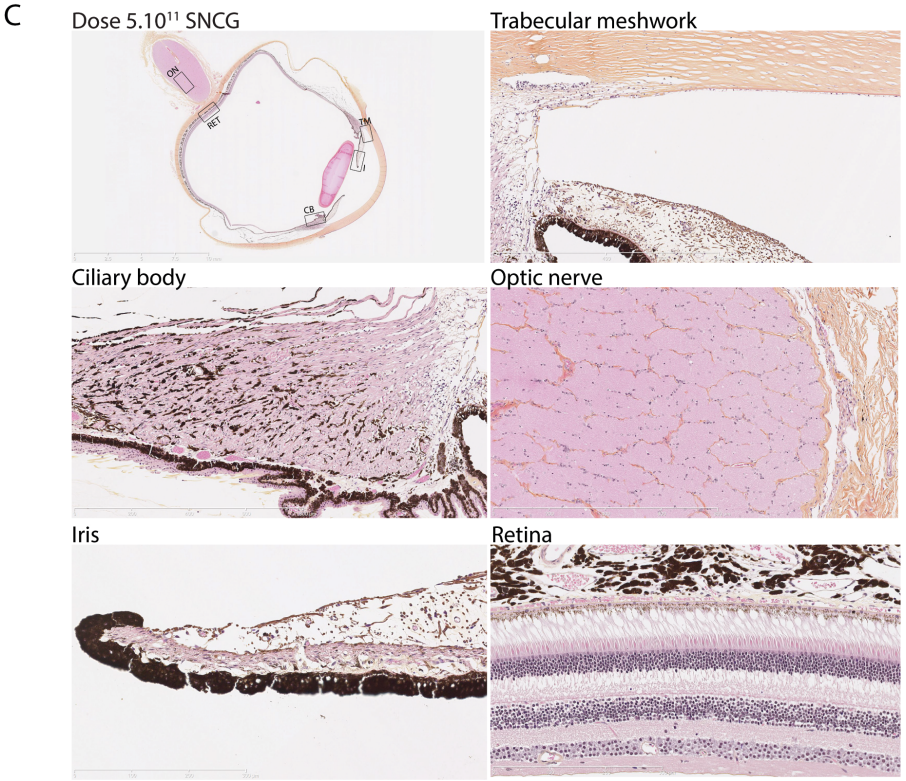
C
Dose 5.10¹¹ SNCG
Trabecular meshwork
Ciliary body
Optic nerve
Iris
Retina
ON
RET
TM
CB

Figure 3- In vivo imaging, ophthalmic exams and histopathology in AAV2-CatCh injected NHPs

A) Fluorescence fundus images of NHP1 injected with low (left) and high dose (center) AAV2-SNCG-CatCh-GFP respectively. OCT scan of high dose eye. Images were obtained at two months post-injection. Fluorescence around the fovea (white arrow) is only visible in the high dose injected left eye. Scale bars: 500 μm. B) Uveitis and level of vitreous haze scores for eyes of all 10 NHPs injected with low (10^{11} vg), mid-dose ($5x10^{11}$ vg) and high dose (10^{12} vg) injections of AAV2 encoding CatCh under SNCG or CMV promoters. C) Histo-pathological examination of the eye from a NHP3 with mid-dose injection of AAV2-SNCG-CatCh at three months post-injection (eye indicated with a white arrow in B) Retinal slice across the vertical meridian of the eye imaged at a resolution of 40x. Absence of detectable lymphocytes, macrophages or damage to ocular structures in the trabecular meshwork, ciliary body, optic nerve, iris and retina on magnified areas.

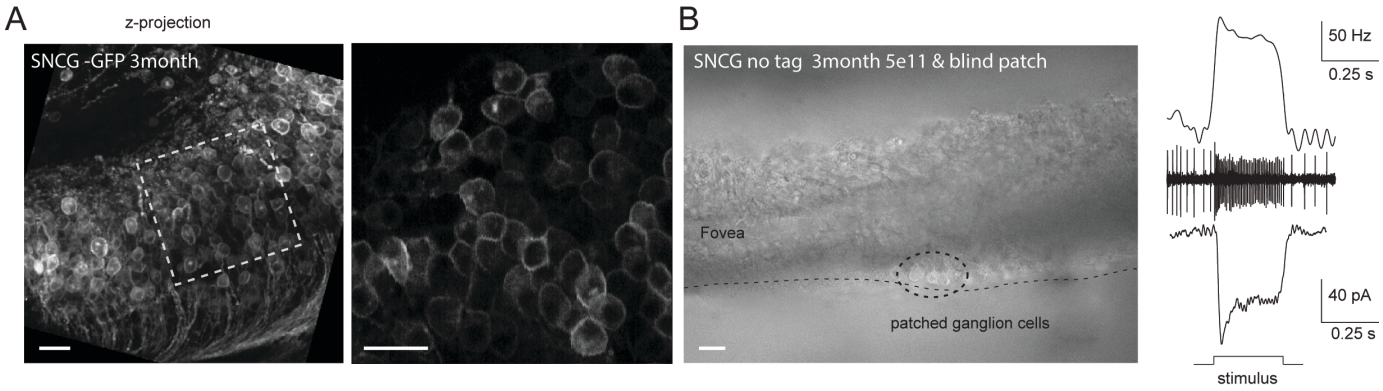
A
z-projection
SNCG -GFP 3month
B
SNCG no tag 3month 5e11 & blind patch
Fovea
patched ganglion cells
50 Hz
0.25 s
40 pA
0.25 s
stimulus

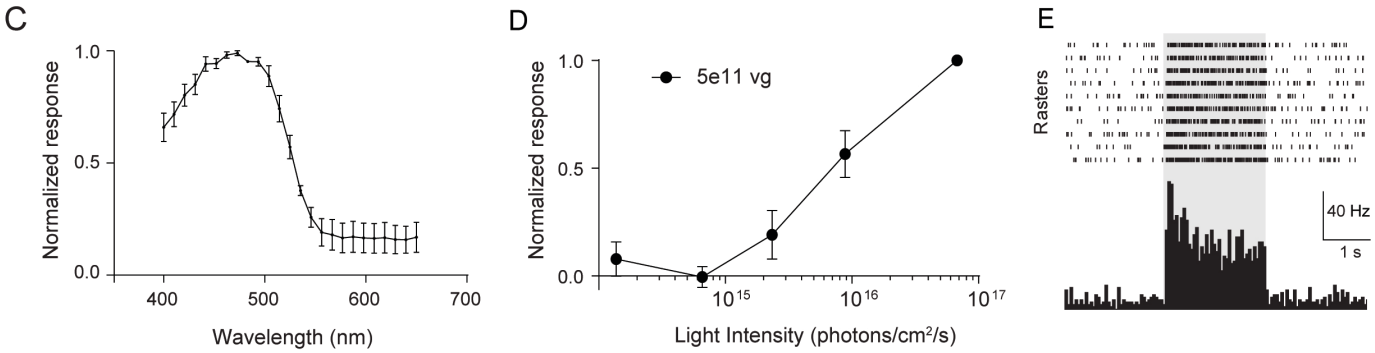
C
Normalized response
1.0
0.5
0.0
400
500
600
700
Wavelength (nm)
D
Normalized response
5e11 vg
1.0
0.5
0.0
10^15
10^16
10^17
Light Intensity (photons/cm²/s)
E
Rasters
40 Hz
1 s

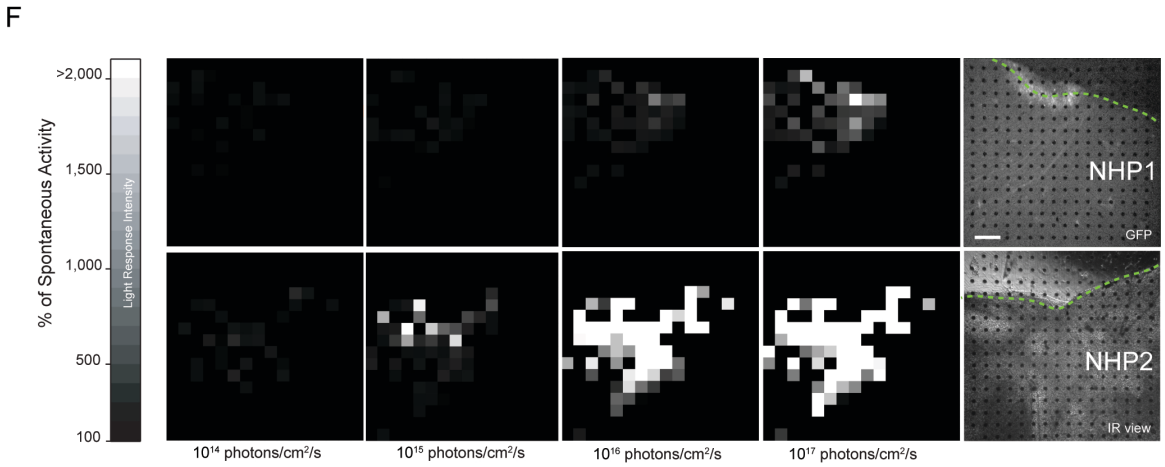
F
% of Spontaneous Activity
>2,000
1,500
1,000
500
100
Light Response Intensity
10^14 photons/cm²/s
10^15 photons/cm²/s
10^16 photons/cm²/s
10^17 photons/cm²/s
NHP1
GFP
NHP2
IR view

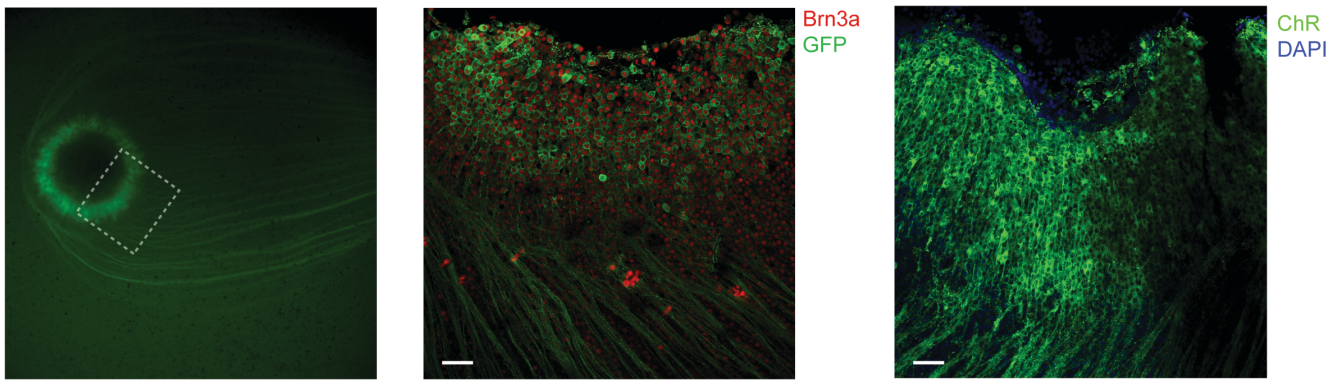
G
H
Brn3a
GFP
I
ChR
DAPI
NHP1
AAV2-SNCG -hCatCh-GFP
NHP2
AAV2-SNCG -hCatCh

Figure 4- Characteristics of CatCh-mediated light responses at three months post-injection

A) Two-photon images of the peri-foveolar region of NHP 1, injected with AAV2-hCatCh-GFP displaying the high density of transfected cells with membrane bound expression. The white dotted square on the left indicates the area displayed at higher magnification on the right. B) Retinal slice showing the peri-foveolar region of NHP 2, injected with AAV2-hCatCh (no GFP tag), where light-responsive ganglion cells were recorded. Recordings in the cell-attached mode show spikes and their increase in frequency during light stimulation. Typical spiking response and photocurrent of cells recorded in cell-attached or whole-cell patch-clamp configuration, respectively. Scale bars (A, B): 20 µm. C) Average spectral tuning at 10^{17} photons/cm2/s after application of L-AP4 in primate retinas expressing hCatCh. D) Average normalized response to different stimulus intensities. E) Raster plot and peri-stimulus time histogram of ganglion cell responses to full field flashes at 480nm, after application of L-AP4 in primate retina injected with AAV2-SNCG-hCatCh-GFP. F) Gray scale maps based on firing rates of responding neurons (expressed as a percentage of their spontaneous activity) at increasing light intensities in primate retinas injected with AAV2-SNCG-hCatCh-GFP (top) and AAV2-SNCG-hCatCh (bottom) at a $5x10^{11}$ vg per eye dose. The macular area is indicated by dashed green line and the black dots represent the locations of the MEA recording electrodes. Scale bar: 200 µm. G) The macular region of NHP1 prior to dissection showing CatCh expression in the peri-foveolar ring. H) Half of the foveal ring as indicated by the white rectangle in G), after MEA recordings and RGC immunolabelling. Retinal flat-mount has been stained with Brn3a (red) and GFP antibodies (green). I) The foveal region of retina from NHP2 (shown in lower right panel of F) after labeling with antibodies against channelrhodopsin (green). Nuclei have been stained with DAPI. Scale bars (H, I): 50 µm. Error bars represent SEM.

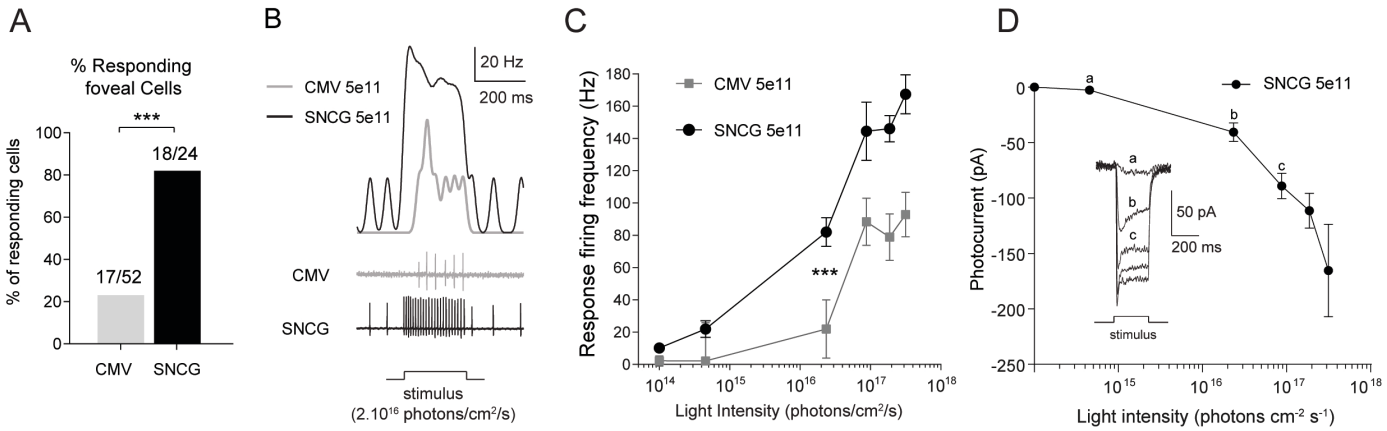
A
% Responding foveal Cells
***
18/24
17/52
% of responding cells
CMV
SNCG
B
CMV 5e11
SNCG 5e11
20 Hz
200 ms
CMV
SNCG
stimulus
(2.10^16 photons/cm²/s)
C
CMV 5e11
SNCG 5e11
Response firing frequency (Hz)
***
Light Intensity (photons/cm²/s)
D
SNCG 5e11
Photocurrent (pA)
a
b
c
50 pA
200 ms
stimulus
Light intensity (photons cm-2 s-1)

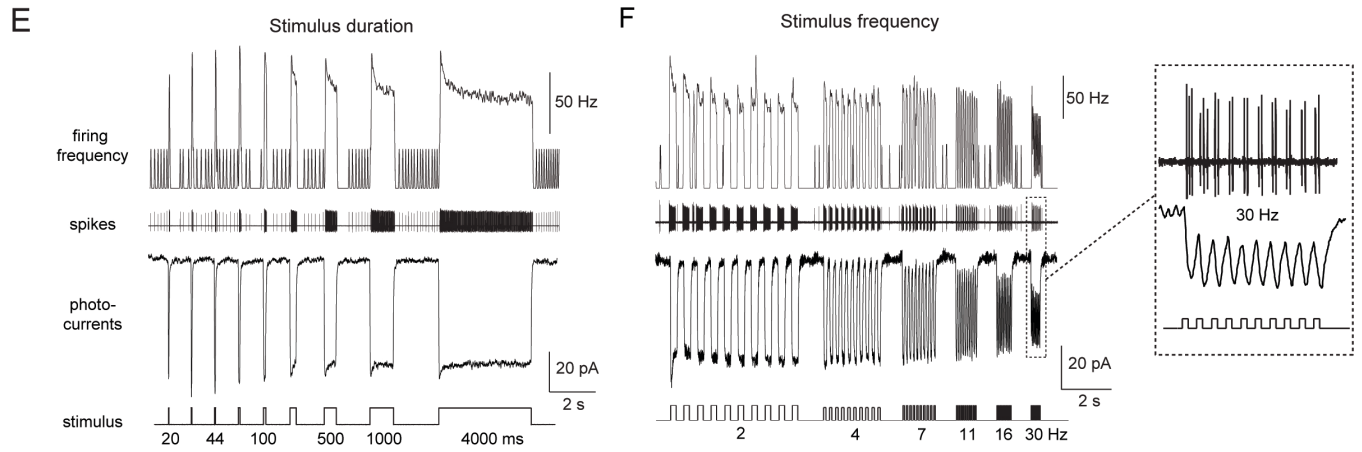
E
Stimulus duration
firing frequency
spikes
photo-currents
stimulus
50 Hz
20 pA
2 s
20
44
100
500
1000
4000 ms
F
Stimulus frequency
50 Hz
20 pA
2 s
30 Hz
2
4
7
11
16
30 Hz

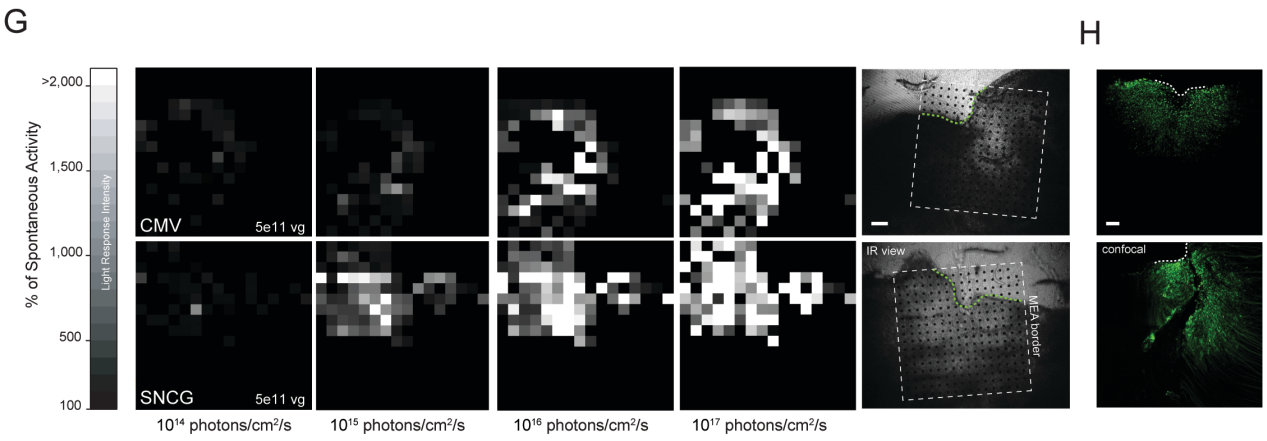
G
H
% of Spontaneous Activity
>2,000
1,500
1,000
500
100
Light Response Intensity
CMV
5e11 vg
SNCG
5e11 vg
IR view
MEA border
confocal
10^14 photons/cm²/s
10^15 photons/cm²/s
10^16 photons/cm²/s
10^17 photons/cm²/s

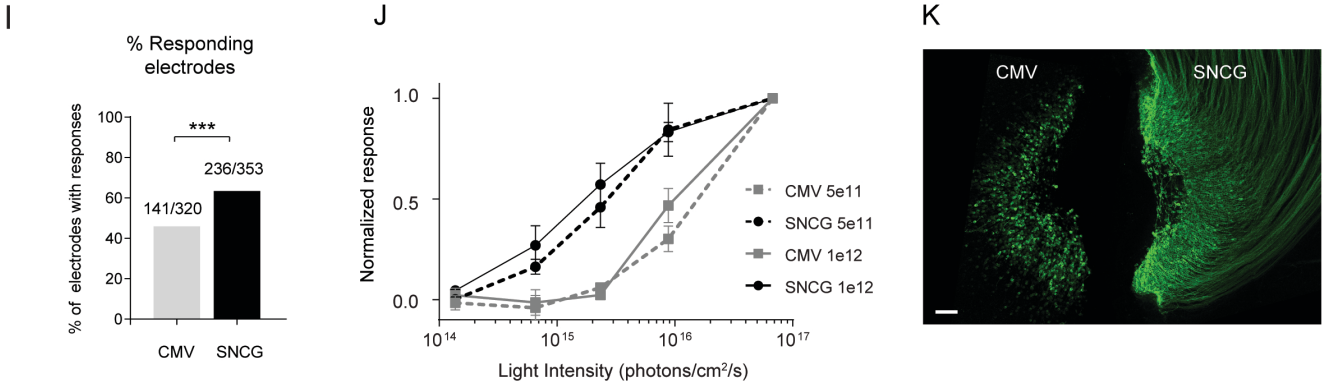
I
% Responding electrodes
***
236/353
141/320
% of electrodes with responses
CMV
SNCG
J
Normalized response
CMV 5e11
SNCG 5e11
CMV 1e12
SNCG 1e12
Light Intensity (photons/cm²/s)
K
CMV
SNCG

Figure 5- Characteristics of CatCh-mediated light responses at six months post-injection

A-F) Results from single cell recordings (using cell-attached and whole-cell patch-clamp configurations) of ganglion cells recorded in the peri-fovealar region of retinas injected either with CMV-CatCh or SNCG-CatCh at a dose of 5 x 10^{11} vg, after application of L-AP4. A) Comparison of the proportions of responsive cells recorded either from CMV-CatCh or SNCG-CatCh. B) Representative recordings showing the spiking frequency obtained for SNCG-CatCh compared to CMV-CatCh (bottom, raw data; top, rate evolution curves) during light stimulation (intensity 2.10^{16} photons/cm^2/s, wavelength 480 nm). C) Response firing frequency of RGCs as a function of light stimulation intensity, for CMV-CatCh and SNCG-CatCh at 5 x 10^{11} vg viral dose. D) CatCh photocurrents (inward currents recorded at -60mV in whole cell configuration) of RGCs as a function of light stimulation intensity, for SNCG-CatCh at $5x10^{11}$ vg per eye. Photocurrents of a representative cell are shown under the intensity-curve. E) Response characteristics to varying stimulus duration. Middle and top row show raw data (cell-attached) of the spiking activity and firing frequency in response to stimuli of increasing duration (20 ms to 4 s). Bottom, photocurrent recorded in whole cell configuration from another representative cell using the same pattern of stimulation. F) Response characteristics to varying stimulation frequencies. Middle and top rows show raw data (cell-attached) showing the spiking activity of a cell and its firing frequency in response to stimuli of increasing frequencies (2 to 30 Hz). Bottom, photocurrents recorded in another representative cell using the same pattern of stimulation. A magnified trace is shown at 30 Hz displaying the robust photocurrents and spiking activity obtained for each of the 10 successive stimulations.

G-K) Results from MEA recordings and histology. G) Gray scale maps based on firing rates of responding neurons (expressed as a percentage of their spontaneous activity) at increasing light intensities in primate retinas injected with AAV2-SNCG-hCatCh-GFP (top) and AAV2-SNCG-hCatCh (bottom) at a $5x10^{11}$ vg per eye, after application of L-AP4. Right, the MEA chip perimeter is represented by a dotted white square, and the putative fovea area is indicated by dashed green curves in the pictures. The black dots represent the locations of the MEA recording electrodes.Scale bar: 200 µm. H) The same foveal regions after MEA recordings and RGC immunolabelling. Retinal flat-mount has been stained with antibodies against channelrhodopsin (green). Note that the SNCG

retina was partially damaged while handling the tissue after MEA procedures. Scale bar: 100 µm. I) Percentage of responsive MEA electrodes for each promoter at $5x10^{11}$ vg per eye. J) Normalized responses of RGCs to light at increasing intensities at 6 months post-injection. Each line represents discharge frequencies normalized across retinas for high dose group (n=2 retinas) and for low dose group (n=3 retinas). K) Foveal regions of 2 representative NHP retinas having received 10^{12} vg dose of AAV-CatCh expressed under CMV (left) or SNCG (right) promoter, after MEA recordings and immunolabelling. Retinal flat-mount has been stained with antibodies against channelrhodopsin (green). Scale bar: 100 µm.

Error bars represent SEM.

A.

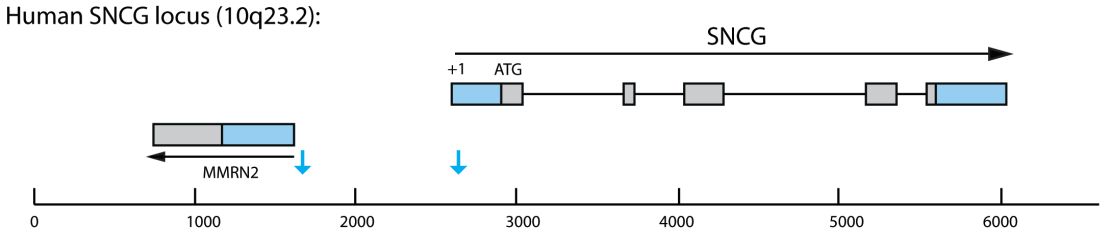

B.

CACCCACAAGCCAGTTCCTGTCCCTGAGGACTTGGCTCAGGGACTCTGGGAATGTGGTAGA
CATGGGGTGGCCCCACCAAATGCATCCTTATGGGAACCTGCTCCCTGGGAGCCATGAAAAGA
GCGTGGACTTCGAGGTGGGGCCACAGGAAGTGGTCAGGTCCATCTCAGGGGACCTGCTGCC
CATCCACACTGCTGGCCAGGAAATGGGGGGCAATTCATGCCTCCTCAGCACCTTCAGCACTG
GGCGGCTCAAAGAAGGCAAGGGACTATTCTGGGGTCACACAGCATGCAGCCAGAGGCCAAG
GCATGAGGAAGTCCTTCATTTCCCCACCCCCACCCACCTCAGATCCTCCAACCGGTTTCATGG
CAGCCCAGGGTCCAGCGGCATCCAGGATGCTGGTGGGTAGCTGCACAGCCCAGGCCGCGGG
AGGTTGGCTGCTCTCACCTAACAGGCCTATGTGGCCCTGACCCCTACCTAGGAAGCTGGGGAC
AATGGCCAAGGCGCCTCCCCTCTCTGTGCCTGTCTGTCCAGGTGCAGCATAGACACAGCACCC
CTGGGGCCAAGAGCACCCAGCCAGGGCTGCCCCCATGGGTGGGCAGGGCAGTAAATGAATGA
GGGACAGGTTGGGAGGTGGCCAGCCCCCTCCAGCCCATGGAGGGCACGGGGCAGGAGAGCT
GGGCTGAGCCAGCAGGAGCCCAGGGAGCCTGGTCTCTGCCTTCCTATCCTGGAGGAAGGTGA
GGCTGAACCTCCTTCCCTCCCTCCCTCCCTCCCCGCCCCCACTGCACGCAGGGCTGGCTGGG
CTCCAGCTGGCCTCCGCATCAATATTTCATCGGCGTCAATAGGAGGCATCGGGGACAGCCGCTG
CGGCAGCACTCGAGCCAGCTCAAGCCCGCAGCTCGCAGGGAGATCCAGCTCCGTCCTGCCTG
CAGCAGCACAACCCTGCACACCC

C.

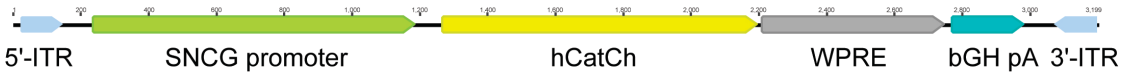

Figure S1- SNCG and AAV construct

A) Schematic representation of the SNCG gene and promoter sequence. The SNCG gene is located on chromosome 10 (10q23.2). It contains 5 exons extending over 3,5 kb from +1 transcription start site to the end of the 5th exon. The blue "boxes" represent non-translated regions. The 1st exon of the multimerine 2 gene (MMRN2) is located 863 bp upstream of +1 SNCG transcription start site, in reverse orientation and only the first exon of MMRN2 is shown in this diagram. In order to extract the human sequence of the SNCG promoter we amplified from HEK-293T cells genomic DNA the -785 to +163 region (indicated by blue arrows), thus containing the 5' untralslated region (UTR) of the SNCG gene. The PCR product was then subcloned into pENTR-D/TOPO and sequenced. The sequence was identical to the Genebank sequence with GeneID6623. This amplified region contains the promoter but no additional promoter characterization has been done within this region. B) Sequence of the SNCG promoter. C) Schematic representation of the AAV construct including CatCh and all the cis-regulatory elements.

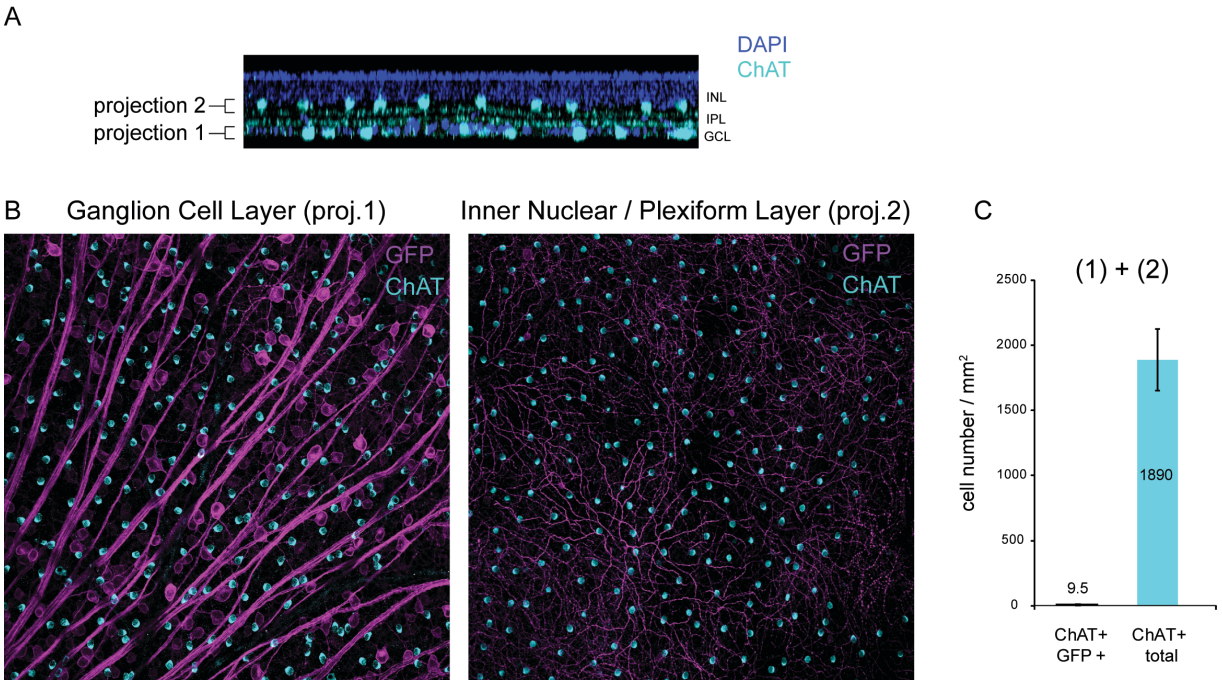

Figure S2- ChAT (Choline-acetyl-transferase) and GFP staining in rd1 mouse retina transduced with AAV2-SNCG-CatCh-GFP

A) Vertical re-slice of confocal horizontal stacks of a retinal flatmount from a representative rd1 retina expressing GFP under the control of SNCG promoter. Nuclei have been stained with DAPI (blue) and amacrine cells have been labeled with ChAT (cyan) antibodies. Z-stack projections 1 and 2, are centered on ChAT+ amacrine cells in the ganglion cell layer and inner nuclear layer (both displaced and non-displaced).

B) Representative confocal z-stack projections across the areas shown in A (proj.1 and proj.2), and co-labeled with ChAT (cyan) and anti-GFP (magenta) antibodies.

C) Quantification of amacrine cells (ChAT+) co-stained with GFP and total number of amacrine cells (in cell number per mm^2) across the two ChAT+ layers (n=4 eyes).

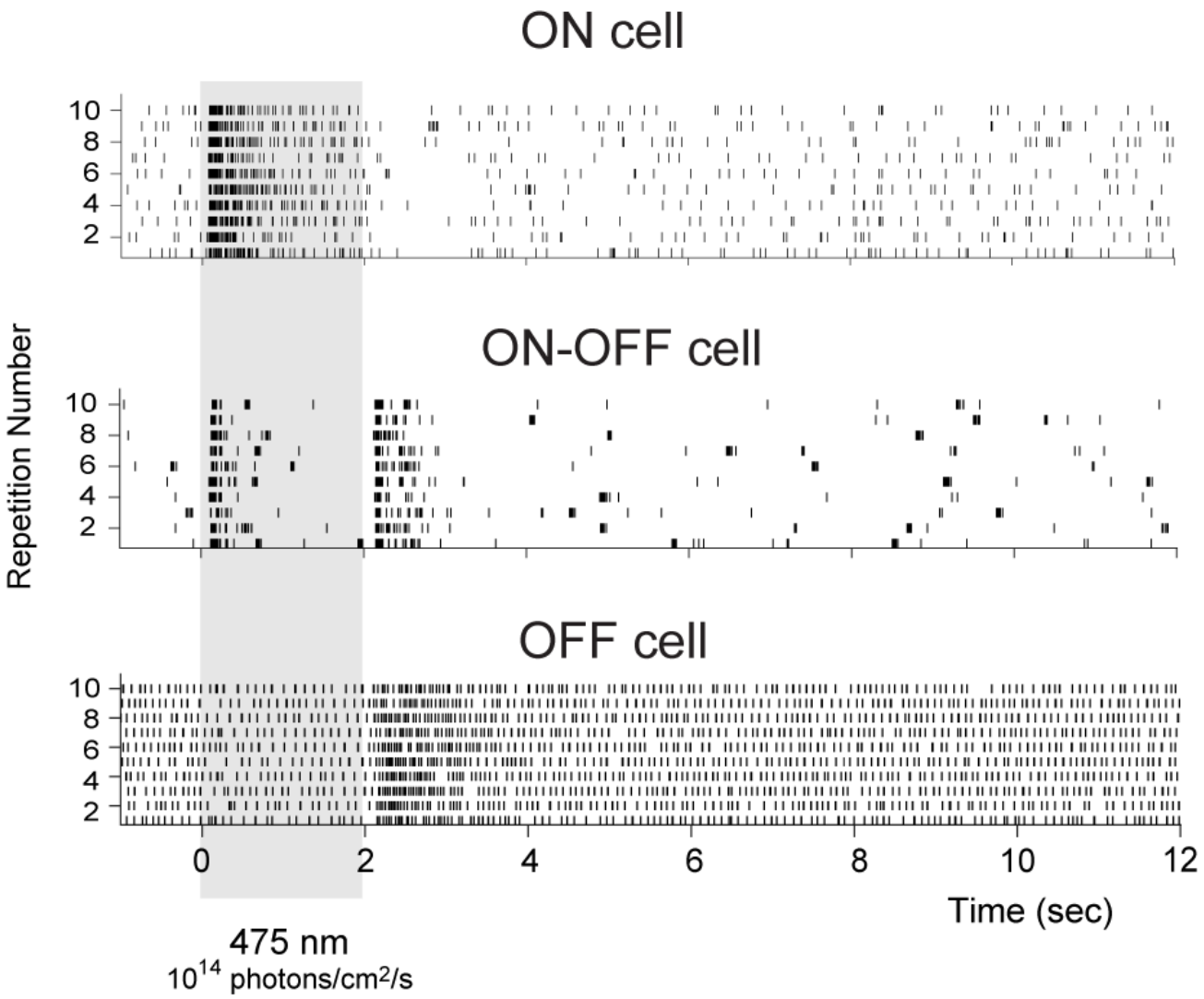

Figure S3- Examples of light responses obtained in wild-type mouse ganglion cells

Raster plots (10 repetitions) from 3 different ganglion cells recorded simultaneously with MEA, displaying ON, ON-OFF and OFF cell responses. Upper panel: ON cell responding to light increments; middle panel: ON-OFF cell, responding to both light increments and decrements; bottom panel: OFF-cell, responding to light decrements. Responses were generated by 2 s long stimulations (indicated in gray) with blue light (475nm) at an intensity of 10^{14} photons/cm^2/s.

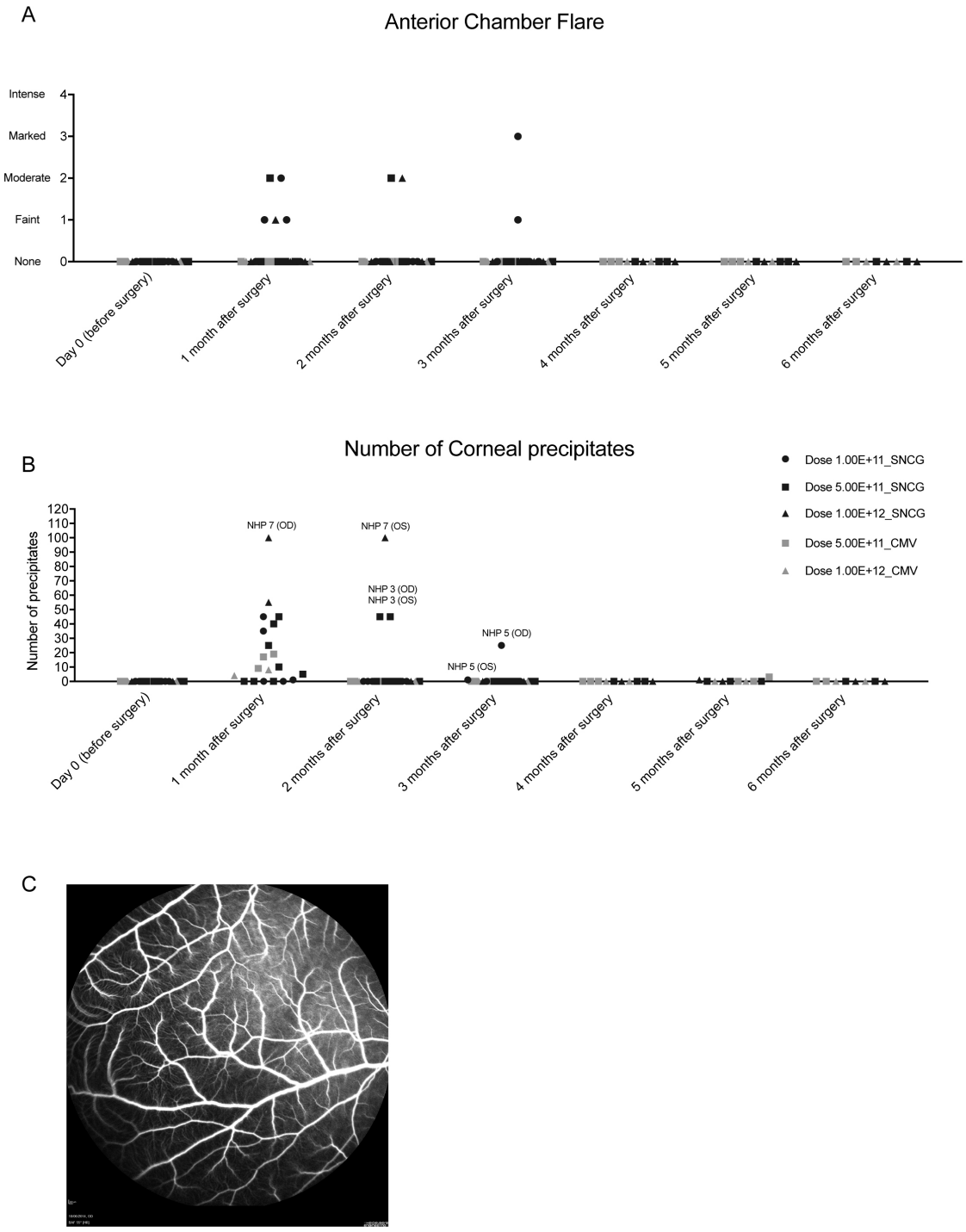

Figure S4- Supplementary ophthalmic exams in AAV2-CatCh injected NHPs

A) Anterior Chamber flare score and B) number of corneal precipitates for eyes of all 10 NHPs injected with low (10^{11} vg), mid-dose ($5x10^{11}$ vg) and high dose (10^{12} vg) injections of AAV2 encoding CatCh under SNCG or CMV promoters. C) Angiography images of NHP3 obtained using enhanced-depth imaging (EDI) techniques combined spectral-domain OCT. Image was selected from the late phase (10 minutes post

intravenous fluorescein injection) of the dye transit; 3 months post AAV injection and no fluorescein leak was observed.

Tables:

NHP #		AAV vector	Dose (vg/eye)	Age	Sacrifice
NHP 1	Right eye	AAV2-SNCG-CatCh-GFP	$1x10^{11}$	10	3 months
	Left eye	AAV2-SNCG-CatCh-GFP	$5x10^{11}$		
NHP 2	Right eye	AAV2-SNCG-CatCh	$5x10^{11}$	8	3 months
	Left eye	AAV2-SNCG-CatCh	$5x10^{11}$		
NHP 3	Right eye	AAV2-SNCG-CatCh	$5x10^{11}$	8	3 months
	Left eye	AAV2-SNCG-CatCh	$5x10^{11}$		
NHP 4	Right eye	AAV2-SNCG-CatCh	$1x10^{11}$	4	4 months
	Left eye	AAV2-SNCG-CatCh	$1x10^{11}$		
NHP 5	Right eye	AAV2-SNCG-CatCh	$1x10^{11}$	4	6 months
	Left eye	AAV2-SNCG-CatCh	$1x10^{11}$		
NHP 6	Right eye	AAV2-CMV-CatCh	$1x10^{12}$	9	6 months
	Left eye	AAV2-CMV-CatCh	$1x10^{12}$		
NHP 7	Right eye	AAV2-SNCG-CatCh	$1x10^{12}$	8	6 months
	Left eye	AAV2-SNCG-CatCh	$1x10^{12}$		
NHP 8	Right eye	AAV2-SNCG-CatCh	$5x10^{11}$	6	6 months
	Left eye	AAV2-SNCG-CatCh	$5x10^{11}$		
NHP 9	Right eye	AAV2-SNCG-CatCh	$5x10^{11}$	16	4,5 months
	Left eye	AAV2-CMV-CatCh	$5x10^{11}$		
NHP 10	Right eye	AAV2-CMV-CatCh	$5x10^{11}$	6	6 months
	Left eye	AAV2-CMV-CatCh	$5x10^{11}$		

Table1- Intravitreal injections in non-human primates indicating the number of the primate, the vector used, dose and the time after the injection.